TAPHONOMY OF THE ORDOVICIAN SOOM SHALE *LAGERSTÄTTE*: AN EXAMPLE OF SOFT TISSUE PRESERVATION IN CLAY MINERALS

by SARAH E. GABBOTT

ABSTRACT. The late Ordovician Soom Shale of South Africa contains exceptionally preserved fossils of several taxa, the soft tissues of which are uniquely composed of clay and alunite group minerals. In addition, originally phosphatic brachiopod shells and conodont elements have been replaced by clays. Sub-cellular structural details of conodont muscle tissues are faithfully replicated by the clay minerals. Geochemical analyses have constrained interpretation of the conditions in the sediment and bottom waters of the Soom Shale basin during deposition and early diagenesis. Anoxic-euxinic conditions prevailed with low carbonate and iron concentrations in the sediment; hence there was no mechanism to buffer or fix H_2S produced by organic matter decomposition. Under low pH conditions and in the presence of cations, organic substrates would have had an affinity for colloidal clay minerals and may have acted as templates, controlling the absorption of clay minerals which eventually completely replaced them. An initial phase of mineralization involving phosphate, followed by its replacement by clay minerals, is unlikely because the low pH conditions in the sediment would have been inimical to phosphate concentration, and the high fidelity of some soft tissue replication militates against two phases of replacement.

THE preservational history of fossils from the Soom Shale is complex. A variety of minerals was involved in replacing and/or replicating fossil material and there was more than one phase of demineralization of the original biominerals. The transformation of normally labile tissues to mineralized replacements was controlled not only by decay of the organisms themselves, but also by the geochemistry of the sedimentary environment. Some soft tissues, notably the myotomes of a conodont animal, preserve structures on a sub-cellular scale of resolution (Gabbott *et al.* 1995). In other parts of the fossil record, comparable replacement of organic structures involves phosphate mineralization, but the Soom Shale specimens are uniquely preserved through replacement by clay minerals (Gabbott *et al.* 1995). The main aim of this paper is to describe the taphonomy and early diagenesis of the Soom Shale biota with special emphasis on the mechanism of preservation of soft tissues. The mode of preservation of the various fossil components in a deposit can provide valuable evidence of the conditions which contributed to their preservation. In particular, authigenic mineral species are indicative of specific depositional conditions such as levels of Eh, pH, organic content, rate of burial, salinity and degree of oxygenation (Allison 1988*a*). A subsidiary aim, therefore, is to use the taphonomic information to help determine the environment of deposition in the basin, the Eh/pH of the bottom and pore waters, and the level of oxygenation at and above the sea floor. In addition, the relative timing of diagenetic processes resulting in mineral transformations has been determined. The effects of Neogene weathering on the preserved assemblage are also noted.

STRATIGRAPHY, LOCALITIES AND SEDIMENTOLOGY

The Soom Shale is the basal member of the Cedarberg Formation which is part of the Lower Palaeozoic Table Mountain Group (Theron and Thamm 1990). The stratigraphy of the Lower Palaeozoic of South Africa has been reviewed by Rust (1981) and aspects of the Cedarberg Formation were described by Cocks *et al.* (1970) and Theron *et al.* (1990). Good fossiliferous

[Palaeontology, Vol. 41, Part 4, 1998, pp. 631–667]

exposures of the Soom Shale occur at Keurbos (18°58′ E, 32°16′ S) near Clanwilliam, and at Sandfontein (19°14′ E, 32°40′ S) 52 km from Clanwilliam. Two cores have been drilled by the Geological Survey of South Africa close to the Keurbos locality, one 5 m behind the Keurbos quarry face, and the other in a stream section approximately 1 km south-west of the quarry.

The Soom Shale comprises a fine siltstone and mudstone laminated on a millimetric scale. It has been subject to Neogene weathering which in most areas has changed it from an original black, as at Sandfontein, to yellow-brown; at Keurbos, it is grey. The most obvious primary sedimentary structure is the fine-grained lamination which is occasionally interrupted by thicker homogenous siltstones up to 10 mm thick. The laminae comprise alternations of silt and mud with darker layers which may be degraded organic matter. The lamination may have been formed by intercalation of distal turbidites with hemipelagites (Jan Zalasiewicz, pers. comm. 1996). However, as shown by the lack of bedding structures, the turbidite flows must have lost most of their energy. Penetrative and surface bioturbation structures are absent. The sediment is composed mostly of clay minerals, especially illites and mixed-layer clays, and detrital quartz. Diagenetic minerals include pyrite, chlorites and clay minerals.

The setting of the basin at the time of deposition of the Soom Shale has been described as glaciolacustrine to shallow marine (Theron *et al.* 1990). Water depth is unknown but cannot have been very great as the Soom Shale overlies the Pakhuis Formation tillites with glacial pavements, and is overlain by the Disa Siltstone Member which is dominantly shallow marine (Rust 1967, 1981). However, there are no indications of storm-wave induced sedimentary structures which may ripple the sediment under water depths of up to 100 m during moderate storms (Elliot 1991). It is therefore likely that a depth of 100 m must have existed over the majority of the depobasin unless the sediment was bound by microbial mats or the sea surface was ice covered. Evidence for periodic ice-coverage comes from the presence of dropstones in the shale particularly towards the base (Rust 1967). However, the climate at the time was generally one of amelioration, resulting in retreat of the ice sheet responsible for the underlying tillites and diamictites.

BIOTA

The palaeontology of the Soom Shale has been examined by a number of authors (Cramer *et al.* 1974; Gray *et al.* 1986; Moore and Marchant 1981; Kovács-Endrödy 1986; Theron *et al.* 1990; Chesselet 1992; Aldridge and Theron 1993; Aldridge *et al.* 1994; Braddy *et al.* 1995; Gabbott *et al.* 1995; Fortey and Theron 1995). Trace fossils are rare but include a variety of faecal pellets. The microbiota includes chitinozoans (Cramer *et al.* 1974), acritarchs and spores (Gray *et al.* 1986). Metaphyte algae cover most of the lamination surfaces and probably constituted the greatest biomass of the biota. It is not yet clear whether the algae were benthonic, and thus stabilized the sediment, or planktonic. At present, the evidence of dominantly inhospitable bottom water conditions favours the latter.

MATERIAL AND METHODS

The repository of most specimens (prefixed C) used in this study is the Geological Survey of South Africa. Specimen numbers prefixed IT are at The Natural History Museum, London.

Fossil analyses

The fossils (Table 1) were studied in two ways; firstly by observation, noting the mode of preservation, degree of compaction and fracturing, presence or absence of biominerals, presence or absence of hard part or soft tissue structures and fidelity of soft part replication, and secondly by determination of the mineralogy of hard parts and soft tissues where present. Biomineralized tissues were investigated on the following material: orthocone shell, lingulate brachiopod shell, trilobite exoskeleton, ostracode carapace and conodont elements. More refractory organic biomolecules

TABLE 1. Fossils from the Soom Shale with their original composition, fossil composition and mode of preservation indicated. ill. = illite and alun. = alunite group minerals.

Fossils	Original composition	Fossil composition	Mode of preservation
Orthocone	Calcium carbonate $CaCO_3$ (aragonite)	—	Mouldic
Trilobite	Outer calcite, inner calcite in organic base $CaCO_3$ (calcite)	—	Mouldic + possible replacement
Lingulate brachiopods	Chitinophosphatic; apatite with 11–42 per cent. organic (chitin and protein)	ill./alun.	Mouldic + replacement
Conodont elements	Calcium phosphate (apatite)	basal bodies, ill./alun. denticle cores, quartz	Mouldic + replacement
Naraoiid	Chitinous	—	Mouldic
Eurypterid exoskeleton	Chitinous	ill./alun.	Replacement
Chitinozoan	Pseudochitin	illite and coalified organic	Replacement and coalified original
Acritarchs + spores	Sporopollenin	coalified organics	Coalified original
Conodont muscle tissue	Labile organic	illite	Replacement
Siphonacis parva	Unknown	organic and alun.	Original and replacement

investigated were from naraoiid carapace, chitinozoan vesicles, conodont sclerotic eye capsules, eurypterid cuticle and *Siphonacis parva* (Kovács-Endrödy), a small enigmatic needle-shaped fossil (Chesselet 1992). Labile soft tissues examined were from the trunk musculature of the conodont *Promissum pulchrum* (Kovács-Endrödy) and eurypterid podomere musculature.

The fossil material was studied by combinations of optical microscopy, SEM EDX (scanning electron microscope energy dispersive X-rays) and electron microprobe (JEOL JXA-8600 microprobe). All specimens used in compositional analyses are shown in Table 2.

There were some difficulties in gaining analyses from some fossil material. Great care was taken to ensure that only fossil material was mounted and that it was analysed without contamination from surrounding sediment. All the fossils from the Soom Shale are soft and contained within friable rock, making it very difficult to remove coherent pieces of fossil material. Extraction of conodont muscle tissue was particularly problematical due to its extreme friability. A small amount of EPOTEK resin dropped directly on to the fossil and allowed to dry for 24 hours proved an effective consolidant. However, some fossil material is so soft that it would not take a sufficient polish for accurate electron microprobe analysis, even after induration; other compacted fossils (e.g. myodocopid ostracodes, chitinozoan vesicles, conodont sclerotic eye capsules, *Lingula*, *Siphonacis parva* and algal strands) are too thin for a polished section to be prepared. SEM EDX analysis of such thin specimens in the matrix is risky because the beam penetrates up to depths of 5 μm giving spurious analyses incorporating the underlying sediment, although it can be used to test for the presence of minerals in the fossils that are not represented in the matrix.

Although only very small quantities of fossil material are required for these analyses, some Soom Shale fossils are extremely rare, with only one or two specimens known (e.g. scolecodont apparatuses and enigmatic taxa). Until other specimens of these rare fossils are found, destructive analysis has been deferred.

TABLE 2. A, summary of SEM EDX data. Eurypterid material is from: C373I and C874II = prosoma; C427a, C809dI and C874Ib = preabdomen; C373ll, eurypterid muscle tissue from podomere on appendage VI and C809dll, muscle tissue between podomeres 2 and 3 on appendage VI. B, summary of electron microprobe data. Eurypterid material is from: C809a = prosoma; C373 and C731b = preabdomen; C427b = margin of the postabdomen just above the telson. K = Keurbos, S = Sandfontein, B = Buffel's Dome, mt. = muscle tissue.

Fossil	Locality	Total number of analyses	Illite only	Alunite only	Illite and alunite
A					
Orbiculoid					
unlabelled 1	K	7	0	3	4
unlabelled 2	K	3	0	3	0
Eurypterids					
C3731	K	4	1	0	3
C373ll mt.	K	3	0	0	3
C427a	K	2	2	0	0
C809dl	K	2	1	0	1
C809dll mt.	K	2	0	2	0
C874bl	K	2	0	0	2
C874bll	K	2	2	0	0
Conodont muscle tissue					
C721b	S	20	20	0	0
Trilobite					
IT18902	B	7	2	0	5
Ostracods					
C945a	K	5	5	0	0
Chitinozoans					
C732a	K	4	3	0	1
896a	S	11	11	0	0
B					
Orbiculoids					
Unlabelled × 2	K	12	0	2	10
C855	K	9	0	8	1
Trematids					
C412a	K	6	2	3	1
C764a	K	3	2	1	0
C903b	S	3	0	3	0
Eurypterids					
C373	K	9	9	1	0
C427b	K	8	3	5	0
C731b	K	6	3	0	3
C809a	K	7	5	1	1
Conodont muscle tissue					
C721b	S	16	16	0	0

SEM, energy dispersive X-rays (EDX). For SEM EDX analysis, a small piece of fossil material was mounted on to an SEM stub and silver- or gold-coated in a Polaron automatic sputter coater. Uncoated conodont muscle tissue was analysed using a SEM EDX at Medical Sciences, Leicester University, and within an environmental chamber at The Natural History Museum, London. EDX analysis is qualitative and some clay mineral species cannot be determined using these data.

Electron microprobe analysis. Microprobe analyses were performed on fossil sections with a focused beam at 15 Kv. Electron microprobe analyses are quantitative, so cation proportions can be

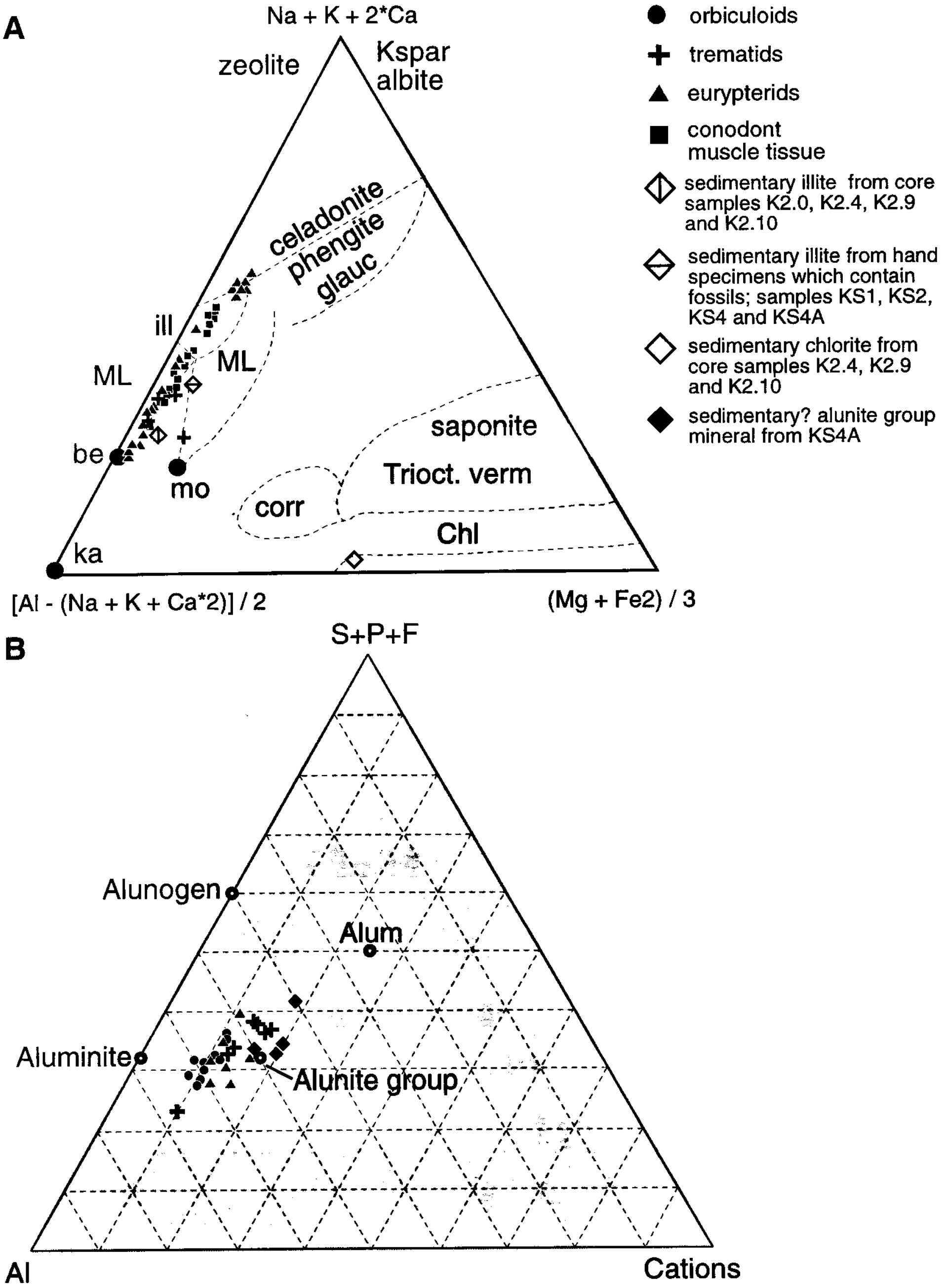

TEXT-FIG. 1. A, Velde and Meunier (1987) diagram for clay minerals showing where the fossil compositions in the illitic solid solution series plot. be = beidellite, Chl = chlorite, corr = corrensite, glauc = glauconite, ill = illite, ka = kaolinite, ML = mixed layer clay, mo = montmorillonite, Trioct. = tricotahedral, and verm = vermiculite. B, triangular plot with anions, cations and aluminium at the apices showing the position of alunitic fossil compositions and the alunite group minerals. Cations: $Fe_2 + Mg + Ca + Na + K + La + Ce + Y + Sr$.

TABLE 3. Mean electron microprobe analyses, standard deviations and cation proportions for fossils with an illitic component (A) and an alunitic group component (B). Ttet = tetrahedral layer total, Toct = octahedral layer total, Tint = interlayer site total.

A	Illitic fossil analyses					
	Eurypterid		Trematid		Conodont muscle tissue	
Oxides	Mean	SD	Mean	SD	Mean	SD
SiO_2	53·47	1·88	49·6	2·3	49·4	1·48
Al_2O_3	34·71	1·06	32	2·62	31·8	2·07
FeO	0·72	0·17	2·06	1·7	0·89	0·13
MgO	1·05	0·06	1·18	0·59	1·38	0·09
CaO	0·12	0·15	0·31	0·38	0·01	0·03
Na_2O	0·15	0·03	0·13	0·04	0·14	0·03
K_2O	5·39	1·14	4·96	0·65	7·27	1·3
P_2O_5	0·19	0·6	0·41	0·78	0	0
Calc total	95·8	2·08	90·7	0·72	90·8	3·02
O equivalents	22		22		22	
	Cations		Cations		Cations	
Si	6·74		6·66		6·68	
AlIv	1·26		1·34		1·32	
Ttet	8·00		8·00		8·00	
AlvI	3·9		3·73		3·75	
Fe^{2+}	0·08		0·23		0·1	
Mg	0·2		0·24		0·28	
Toct	4·18		4·2		4·13	
Ca	0·02		0·04		0	
Na	0·04		0·03		0·04	
K	0·87		0·85		1·26	
Tint	0·93		0·92		1·3	
P_2O_5	0·02		0·05		0	

B	Alunitic fossil analyses					
	Eurypterid		Trematid		Orbiculoid	
Oxides	Mean	SD	Mean	SD	Mean	SD
SiO_2	0·37	0·57	0·24	0·62	0·18	0·17
Al_2O_3	47·09	4·26	39·64	7·12	47·87	4·91
FeO	1·28	0·26	3·17	2·86	1·22	0·62
MgO	0·09	0·03	0·02	0·03	0·03	0·01
CaO	5·09	1·21	5·06	2·90	5·53	0·28
Na_2O	0·90	0·55	0·45	0·69	0·20	0·17
K_2O	3·25	1·66	1·82	2·09	1·21	0·39
La_2O_3	0·05	0·09	0·40	0·37	0·06	0·09
Ce_2O_3	0·41	0·11	1·47	1·10	0·58	0·11
Y_2O_3	0·09	0·07	0·20	0·17	0·01	0·03
SrO	0·77	0·29	1·69	1·20	0·85	0·10
P_2O_5	13·38	4·52	19·36	7·87	12·94	0·66
F	1·22	0·58	1·05	0·44	0·84	0·09
SO_3	22·33	3·06	15·89	6·42	22·14	3·69
Calc total	96·32	2·87	90·44	3·84	93·66	7·19
O equivalents	22		22		22	
	Cations		Cations		Cations	
Si	0·05		0·03		0·02	
Al	6·91		6·33		7·17	
Fe^{2+}	0·13		0·36		0·13	
Mg	0·02		0·00		0·01	
Ca	0·68		0·73		0·75	
Na	0·22		0·12		0·05	
K	0·52		0·31		0·03	
La	0·00		0·02		0·00	
Ce	0·02		0·07		0·03	
Y	0·01		0·01		0·00	
Sr	0·06		0·13		0·06	
P_2O_5	1·41		2·22		1·39	
SO_3	2·08		1·61		2·11	
F	0·48		0·45		0·34	

TABLE 4. Mean electron microprobe analyses, standard deviations and cation proportions for sedimentary samples from the Soom Shale Member. Samples analysed: illites from core specimens K2.0, K2.4, K2.9 and K2.10; chlorites from core specimens K2.4, K2.9 and K2.10; illites from hand specimens with fossils KS1 (C275b), KS2 (C937a), KS4 and KS4A (C907a); alunite group minerals from KS4A (C907a). KS1–KS3 are from Keurbos and KS4 and KS4A from Sandfontein. The negative total charges are probably due to the absence of a Ti analysis. Ttet = tetrahedral layer total; Toct = octahedral layer total; Tint = interlayer site total.

	Illites from core sections		Illites from KS1, KS2, KS4, KS4A		Chlorites from core sections		Alunites from KS4A	
Oxides	Mean	SD	Mean	SD	Mean	SD	Mean	SD
SiO_2	54·02	2·58	52·86	2·33	29·38	1·81	0·11	0·23
Al_2O_3	35·17	2·77	29·96	4·02	21·42	1·17	25·03	4·23
FeO	1·66	0·71	1·87	0·7	23·58	1·19	5·12	0·87
MnO	0·00	0·02	0·01	0·01	0·14	0·13	0·00	0·00
MgO	1·4	0·74	1·53	0·42	13·26	2·08	0·00	0·00
CaO	0·02	0·02	0·08	0·1	0·07	0·04	3·35	0·13
Na_2O	0·24	0·23	0·2	0·18	0·02	0·02	0·18	0·03
K_2O	4·29	1·22	5·1	1·57	0·41	0·26	3·19	0·13
La_2O_3	0·03	0·07	0·00	0·00	0·00	0·00	1·17	0·06
Ce_2O_3	0·00	0·00	0·01	0·03	0·00	0·00	2·62	0·17
SrO	0·00	0·00	0·00	0·00	0·00	0·00	1·43	0·31
P_2O_5	0·01	0·02	0·0	0·11	0·00	0·00	15·42	1·61
SO_3	0·00	0·00	0·06	0·12	0·00	0·00	12·35	1·03
F	0·13	0·12	0·19	0·12	0·00	0·00	0·37	0·21
Calc total	97·22	2·62	91·91	3·48	89·31	0·79	70·34	4·64
O equivalents	22		22		28			22
	Cations		Cations			Cations		Cations
Si	6·71		6·97			6·01	Si	0·02
Al^{IV}	1·29		1·03			1·99	Al	5·45
Ttet	8		8		Ttet	8		
Al^{VI}	3·86		3·63			3·18		
Fe^{2+}	0·17		0·21			4·03	Fe^{2+}	0·79
Mg	0·26		0·30			4·03	Mg	0
Toct	4·29		4·14				Ca	0·66
							Na	0·06
Ca	0		0·01			0·02	K	0·75
Na	0·06		0·05			0	La	0·08
K	0·68		0·86			0·12	Ce	0·18
Tint	0·74		0·92		Toct	11·38	Sr	0·15
P_2O_5	0		0			0·05	P_2O_5	2·41
OH	—		—			—	SO_3	1·71
Total charge	−0·11		−0·19			−0·19	F	0·22

calculated allowing determination of clay mineral species (Text-fig. 1). When using the electron microprobe to investigate mineral chemistries quantitatively, total counts of lower than 85 per cent. are not usually valid and are discarded. However, alunite group minerals, which are important components of some of the Soom Shale fossils, contain structural and free water and would therefore give very low total counts. For this study, therefore, all counts for alunite group minerals have been considered (Table 3).

TABLE 5. Mineralogy of the Soom Shale Member from core sections (K1.1A–K2.14) and hand specimens (K3.0–K3.4) as determined by XRD clay and whole rock analyses.

XRD WHOLE ROCK ANALYSIS	Alunite			●																															
	Pyrite			●	●	●	I	●			●	●	●	●	●	●	●	●	●		I			●			●	I	I	I					
	Kotschubeite						I				●										I		●					I	I	I					
	Chlorite				●		I	●				●	●	●	●	●	●	●	●	●	I	●	●	●	●	●	●	I	I	I					
	Illite	●		●	●	●	I	●	●	●	●	●	●	●	●	●	●	●	●	●	I	●	●	●	●	●	●	I	I	I	●	●	●	●	●
	Quartz	●	●	●	●	●	I	●	●	●	●	●	●	●	●	●	●	●	●	●	I	●	●	●	●	●	●	I	I	I	●	●	●	●	●
XRD CLAY ANALYSIS	Chlorite		●	●	●	●	●		●		●	●	●	●	●	●	●	●	●	●	●	●	●	●	●	●	●	●	I	I	●	●			●
	Kaolinite		●	●	●	●	●	●	●	●	●	●	●	●	●	●	●	●	●	●	●	●	●	●	●	●	●	●	I	I	●	●			●
	Illite	●	●	●	●	●	●	●	●	●	●	●	●	●	●	●	●	●	●	●	●	●	●	●	●	●	●	●	I	I	●	●	●	●	●
	Quartz	●	●	●	●	●	●	●	●	●	●	●	●	●	●	●	●	●	●	●	●	●	●	●	●	●	●	●	I	I	●	●	●	●	●
	Sample	K1.1A	K1.1B	K1.2	K1.3	K1.4	K1.5	K1.6	K1.7	K1.8	K2.0	K2.1	K2.2	K2.3	K2.4	K2.5	K2.6	K2.6A	K2.7	K2.8	K2.9A	K2.9B	K2.10	K2.11	K2.12	K2.13	K2.14A	K2.14B	K2.15A	K2.15B	K3.0	K3.1	K3.2	K3.3	K3.4

Treatment of possible organics from Siphonacis. The needle-like specimens of *Siphonacis parva* appear to have an organic composition. This was tested on a small piece of shale taken from C829 on which the *Siphonacis* are black and unmineralized. The sample was split into two where the preservation of the *Siphonacis* was identical on each piece. One piece was placed into 10% HF overnight to dissolve the matrix and any mineral matter (excepting sulphides). The residue consisted of very small black pieces (1–2 mm long) of indeterminable shape. These were probably broken up pieces of *Siphonacis* and their survival after HF maceration indicates them to be of either organic or sulphide mineral composition. The remaining half specimen was placed into a 10% solution of HNO_3 for three days and showed no sign of alteration in the black *Siphonacis* material. The black material did not oxidize in the nitric acid (a strong oxidizing agent) and is therefore probably organic in composition.

Sediment analyses

Bulk sediment from core sections, hand specimens and fossil-bearing hand specimens was analysed using a variety of techniques (see Tables 4–6).

Sediments analysed show a variation in the degree of weathering. Least weathered are the core samples, but even these sometimes show pervasive shear zones and split easily into discs; therefore, they may have been altered to some degree from an original early diagenetic mineralogy by contact with meteoric waters. Sediment samples from Sandfontein have been similarly affected and, in addition, have been subjected to surface weathering processes, including those induced by percolating meteoric waters. The least pristine sediment samples are from Keurbos, which, in addition to exhumation, have been subjected to deep Neogene weathering and alteration by extensive shear zone fluids. Attempts to constrain the early diagenetic conditions prevalent at the time of dissolution of biominerals and mineralization of soft tissues in the Soom Shale biota can only be conducted on the freshest material. However, mineralogical changes produced by more recent processes must be distinguished because they have an important effect on the final mode of preservation. The identification of minerals produced by weathering also allows more accurate determination of the original early diagenetic mineralogy. Backscatter imaging can be a powerful

TABLE 6. TOC (total organic carbon wt %), % S (sulphur wt %) and DOP (degree of pyritization) for core and hand specimen samples (see Table 5) from the Soom Shale Member.

Sample	Carbon wt %	Sulphur wt %	C/S	DOP	Sample	Carbon wt %	Sulphur wt %	C/S	DOP
K1.1A	2·01	0·77	2·61		K2.7	0·4	2·49	0·16	
K1.1B	0·79	3·68	0·21		K2.8	0·4	0·85	0·47	0·27
K1.2	1·03	3·79	0·27	0·68	K2.9A	0·49	2·31	0·21	
K1.3	0·71	3·87	0·18		K2.9B	0·11	0·18	0·61	
K1.4	0·42	1·53	0·27	0·72	K2.10	0·37	0·96	0·39	0·21
K1.5	0·93	3·39	0·27		K2.11	0·39	0·2	1·95	
K1.6	0·84	3·22	0·26		K2.12	0·33	0·29	1·14	
K1.8	0·23	0·03	7·67		K2.13	0·34	0·36	0·94	
K2.0	1·19	2·51	0·47		K2.14A	0·35	1·07	0·33	
K2.1	0·57	2·48	0·23		K2.14B	0·2	0·16	1·25	
K2.2	1·4	3·27	0·43	0·66	K3·0	0·13	0·26	0·50	
K2.3	0·73	3·91	0·19		K3.1	0·19	0·06	3·17	
K2.4	1·2	4·38	0·27		K3.2	0·09	0·03	3·00	
K2.5	0·76	3·56	0·21		K3.3	0·96	0·04	24·00	
K2.6	0·59	2·73	0·22		K3.4	0·12	0·14	0·86	
K2.6A	0·6	2·83	0·21						

TABLE 7. Summary of the mineralogy of the Soom Shale sediment from core samples, Sandfontein and Keurbos as determined by EM and XRD analyses.

Core samples	Sandfontein	Keurbos
Quartz	Quartz	Quartz
Illite	Illite	Illite
Kaolinite	—	Kaolinite
Chlorite	Chlorite	Chlorite
—	Anatase	Anatase
Apatite	—	—
Pyrite	—	—
Alunite	Alunite	—

tool in determining whether a mineral is detrital or diagenetic (see Macquaker 1994) and will be used in future research. Preliminary backscatter imaging on Soom Shale sediment, however, was not rewarding because the grain size is too fine to be resolved on the available equipment.

Electron microprobe analysis. Polished thin sections were prepared, carbon coated and probed with a focused beam. Samples were chosen to represent a range of lithologies and to investigate the difference in mineralogy between fresh (core samples) and weathered rock from Keurbos and Sandfontein. Owing to the importance of the presence or absence of alunite group minerals, analyses were considered even if total counts were less than 85 per cent. (see Table 4).

X-ray diffraction. X-ray diffraction was carried out on both whole rock and $< 2\ \mu m$ fractions using a Philips PW1729 X-ray generator and PW1710 diffractometer with multiple sample changer. The diffractometer was Ni-filtered with Cu K at 35 Kv, 55 mA. The $< 2\ \mu m$ fractions were run: (1) air dried, (2) following glycolation at 75 °C for 12 hours, and (3) after heating at 550 °C for 1·5 hours.

Total organic carbon and sulphur. Total organic carbon and % sulphur were determined using a LECO CS-125 analyser, using steel standards, after 10% HCl treatment. Samples were identical with those used in XRD analysis (see Table 5).

Degree of pyritization. Degree of pyritization (DOP) is defined as:

$$\mathrm{DOP} = \frac{\%\ \mathrm{Fe\ as\ pyrite}}{\%\ \mathrm{Fe\ as\ pyrite} + \%\ \mathrm{Fe\ HCl}}$$

where the % Fe HCl is the amount of iron liberated on treatment with hot concentrated HCl, and is a measure of the Fe still available that would be reactive to H_2S (see Berner 1970; Raiswell *et al.* 1987). Acid soluble iron was determined by the technique of Berner (1970). This method, using an ICP (inductively coupled plasma-Philips PV8060) has an average precision of 5 per cent. (Raiswell *et al.* 1994). Berner (1970) found the solubilities of iron minerals in HCl (by the method used here) to be similar to their reactivity with H_2S. It should be noted, however, that the concentration of HCl used may lead to solution of greater quantities of iron than would have been available to react with normally low concentrations of H_2S. Thus the DOP values given have a maximum value for % acid soluble iron and consequently provide a minimum value for DOP.

Conventional methods determine the amount of pyrite sulphur and hence pyrite iron (Westgate and Anderson 1982; Canfield *et al.* 1986). These methods are prone to some ambiguity and overlap in the separation of pyrite, elemental sulphur and organic sulphur species (Lord 1982). These ambiguities are eliminated by using an iron based technique as in this study. This procedure not only yields a higher selectivity but allows lower detection limits (Lord 1982). Samples analysed for DOP were from core material only (Table 6) and were chosen as they are all relatively fresh, and represent a wide spread through the Soom Shale sequence. In addition all samples, except K2.8, were known to contain pyrite from XRD analysis (Table 5).

X-ray fluorescence (*XRF*) *whole rock analysis.* Major oxide analyses were determined using the method described by Pickering *et al.* (1993).

Trace element analysis. Trace element analyses were performed on powdered pellets using the methods described by Tarney and Marsh (1991).

RESULTS

Fossil analyses

Eurypterids. Analyses of the exoskeleton by EDX (Text-fig. 2A–C) and electron microprobe have shown it to be composed of illite, alunite or a mix of illite and alunite (Tables 2–3). There is no correlation between the colour of the material (pink, yellow, buff brown or silver) and the presence of illite and mixed-layer clay and/or alunite.

Most eurypterids in the fossil record are exuviae but the preservation of internal muscle tissues in specimen C373 (holotype of *Onychopterella augusti* Braddy, Aldridge and Theron, 1995) shows this specimen, at least, to be the remains of an actual carcass (Braddy *et al.* 1995). Eurypterids from the Soom Shale comprise external and internal moulds but with considerable exoskeletal material present. In all cases, the original complex of chitin and proteinaceous material of the exoskeleton has been replaced by clays and alunite group minerals. Chitin is a polysaccharide carbohydrate and has been shown in decay experiments on the shrimp *Crangon* to be a relatively decay resistant biomolecule, especially when tanned or sclerotized (Briggs and Kear 1994). It is an important component of many non-mineralized marine arthropods which have an extensive fossil record (e.g. Briggs and Clarkson 1989; Butterfield 1990, 1994). However, there is a lack of evidence for the presence of chitin in fossils, suggesting that the preservation of chitinous tissues involves a gradual substitution of chitin by more resistant organic matter (Baas *et al.* 1995).

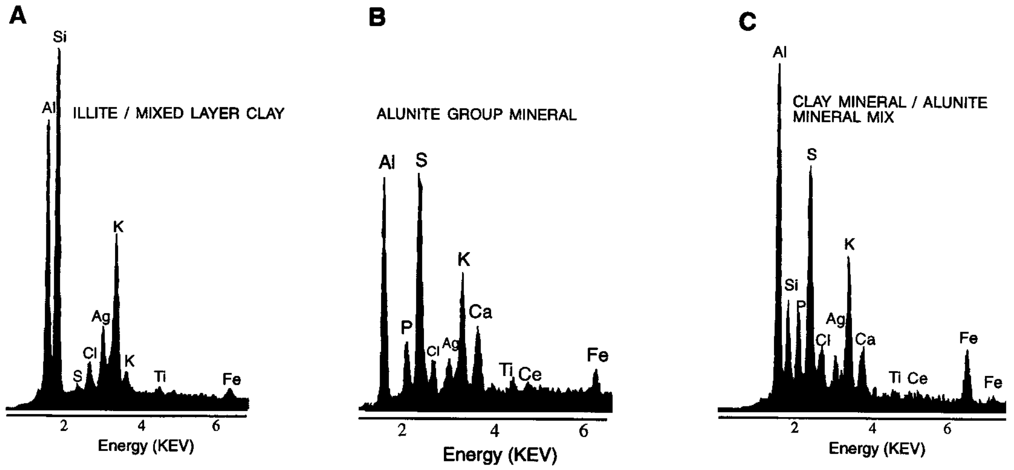

TEXT-FIG. 2. EDX traces of eurypterid specimens from Keurbos. A, cuticle from the prosoma of specimen C809d; B, eurypterid muscle tissue between podomeres on appendage VI from specimen C809d; C, cuticle from the prosoma of specimen C874b.

Trilobites. Specimens of *Mucronaspis olini* Moore and Marchant from the Soom Shale occur as external moulds with no trace of original exoskeleton. The absence of $CaCO_3$ was corroborated by seven EDX analysis which showed pure illitic and mixed illitic and alunitic compositions (Table 2A). Cl was recorded in one analysis and Ce was recorded in one analysis. It is not clear in which mineral phase Cl occurs; Ti probably occurs in the illites and Ce is probably within an alunitic mineral. Trilobite exoskeletons are composed of two layers: an inner layer composed of microcrystalline calcite set in an organic base and an outer thinner layer composed of prismatically arranged calcite crystals (Teigler and Towe 1975). It is unclear whether the illite and alunite grew on the exoskeleton or represent background sediment.

Specimens of the naraoiid *Soomaspis splendida* Fortey and Theron, 1995 preserve little of their original relief. The entire exoskeleton in all specimens shows signs of crushing, especially on the pygidium (Fortey and Theron 1995). Cracks are present on the pygidium and cephalic shield of the holotype (Fortey and Theron 1995). Only the holotype (C453) shows any cuticle preservation, lying anterior to the cephalic margin (Fortey and Theron 1995); other specimens are preserved as internal and external moulds. *Soomaspis splendida* had a non-mineralized cuticle which may have been chitinous (Fortey and Theron 1995).

Orthoconic nautiloids. In the Soom Shale, orthocones are preserved as internal or external moulds, or as composite moulds. Despite the absence of original aragonitic shell material, details of the conchs, such as growth lines and ornament, are evident. All show some degree of flattening. Many of the orthocones are colonized by disciniscid brachiopods. There are three broad styles of conch preservation: (1) retention of some relief and lacking fracture patterns: these conchs were probably filled with sediment prior to compaction; (2) with little of the original relief and with longitudinal fracture patterns in the body-chamber, but chaotic fracture patterns in the phragmocone, produced by crushing; and (3) with body-chambers nearly completely flat with longitudinal wrinkles and the phragmocones severely flattened.

Four orthocone specimens contain radulae in their body-chambers, preserved as external moulds. Radulae were originally composed of chitin (Hunt and Nixon 1981).

Lingulate brachiopods. SEM EDX and electron microprobe analyses of orbiculoid shells from Keurbos show alunite and mixed alunite and illite compositions (Tables 2–3). The orbiculoid shell

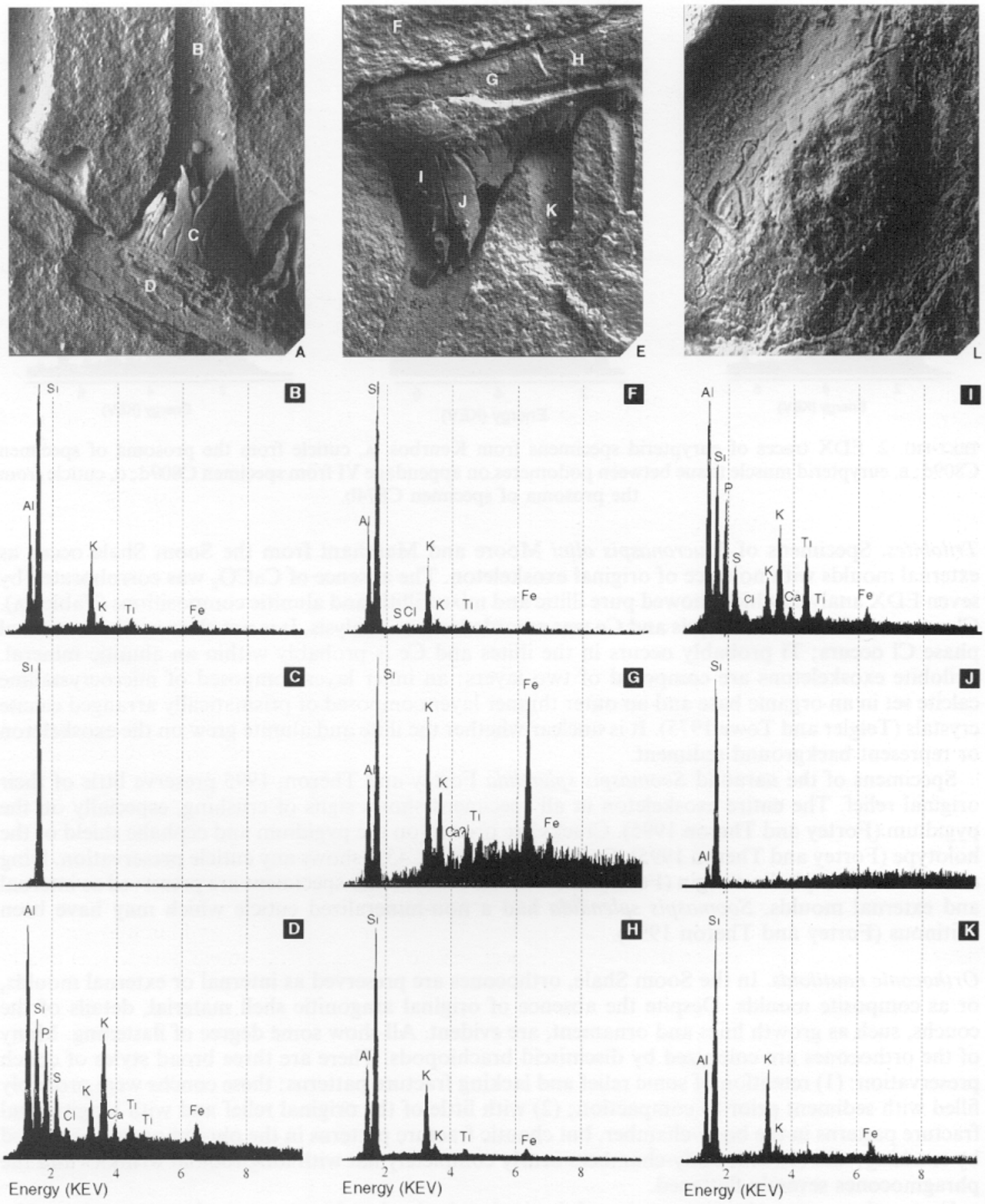

TEXT-FIG. 3. Photographs and EDX traces of conodont S elements and surrounding sediment from Keurbos (C424a). A, basal body/process (bottom), prismatic enamel and mouldic denticle crown; letters B–D denote positions where EDX analyses B–D were taken. E, basal body/process (top), prismatic enamel and mouldic denticle crown; letters F–K denote positions where EDX analyses F–K were taken. L, shows severe dissolution of the denticle and cracking of the basal body/process. A, × 55; E, × 80; L, × 200.

from Sandfontein was composed of alunite only (Tables 2B and 3B). Electron microprobe analyses of trematid shells from Keurbos showed either illite only, alunite only or both minerals (Tables 2B and 3).

Orbiculoids are the most abundant brachiopods in the Soom Shale; they have a complex mode of preservation where internal and external moulds co-occur. Most still retain a high proportion of shell material, particularly on the external surface. Growth lines are clearly distinguishable on the internal surfaces of the valves and fila are apparent on some of the external surfaces. A few shells have solid material in the position of the muscle scars, possibly representing the remains of soft tissues.

Trematids are not nearly so common in the Soom Shale as orbiculoids but show excellent preservation of their radially arranged ornament when found isolated in the sediment, unassociated with orthocones. Isolated trematids are dominantly mouldic and display details of growth lines, but some shell material is preserved. However, where they are found on or in close proximity to orthocones they are flat and very poorly preserved.

Orbiculoids and trematids are disciniscids, having chitinophosphatic shells with an organic content accounting for 25 per cent. of the exoskeletal dry weight (Jope 1965, p. H158). The inorganic phase is dominantly calcium phosphate (75·2% $CaPO_4$) with subordinate amounts of calcium carbonate (8·6% $CaCO_3$) (Williams *et al.* 1992). The shell structure of living and fossil disciniscids has been thoroughly studied by Williams *et al.* (1992). Beneath the periostracum of the disciniscid shells (e.g. *Discinia striata* Schumacher) lies the primary shell consisting of bands representing apatitic and organic concentrations which have many different configurations. Four types of biomineral laminae are distinguishable in the secondary shell, all composed, in varying proportions, of apatite granules (4–8 nm in diameter) with a chitino-proteinaceous coat. The biomineral component of the shells from the Soom Shale has been largely dissolved, but some clay and alunite mineral replacement has occurred.

Conodonts elements. Several elements contain mineralized material in their denticle cores and along the basal bodies and/or processes (Text-fig. 3A, E). Elements from Keurbos only rarely retain such material which is often yellow or pink due to weathering, but may appear black. Survival of mineral material in the elements is more common at Sandfontein. Here, black, shiny mineralized material is most commonly situated in the denticle cores. The distinct preservational mineralogies of the basal bodies, prismatic and aprismatic enamel within the conodont elements (see below), probably reflects differences in the original compositions of these tissues.

The basal bodies/processes of S elements from both Keurbos and Sandfontein show mineral replacements which are commonly fractured and cracked (Text-fig. 3L, from Keurbos). The mineralogy of the basal body in specimen C424a from Keurbos was found to be a mixture of illite and alunite group minerals; EDX analyses are shown in Text-figure 3D (illite and alunite) and 3G–H (illite). A single analysis of the basal body of specimen C679a from Sandfontein gave a dominantly illitic EDX trace.

In all the conodont elements observed, the aprismatic enamel from the denticle crown is absent, resulting in mouldic preservation (Text-fig. 3A, E). The mouldic trace of the aprismatic enamel may be used to delineate its former position in the elements; in some examples, mouldic preservation is seen to occur in the denticle crown and along the edge of the basal body linking separate denticles (Text-fig. 3A, E). The prismatic enamel, when present, shows three styles of preservation. In many of the denticles from Keurbos, the original prismatic structure is present (Text-fig. 3A, E). In three of the four EDX analyses of the prismatic enamel from specimen C424a (Keurbos), excitation peaks corresponding to quartz (± small amounts of Al in two of the three analyses, see Text-fig. 3C, J for two of the EDX traces) were obtained. In a single analysis of the prismatic material from the same specimen (Text-fig. 3I), the composition was of illite and alunite. The prismatic enamel is most commonly preserved by quartz with no trace of apatite. Specimen C679a from Sandfontein shows another mode of preservation of prismatic enamel, in which denticle cores have an outer smooth surface and the prismatic structure is not apparent. Of eight EDX analyses of the denticle core

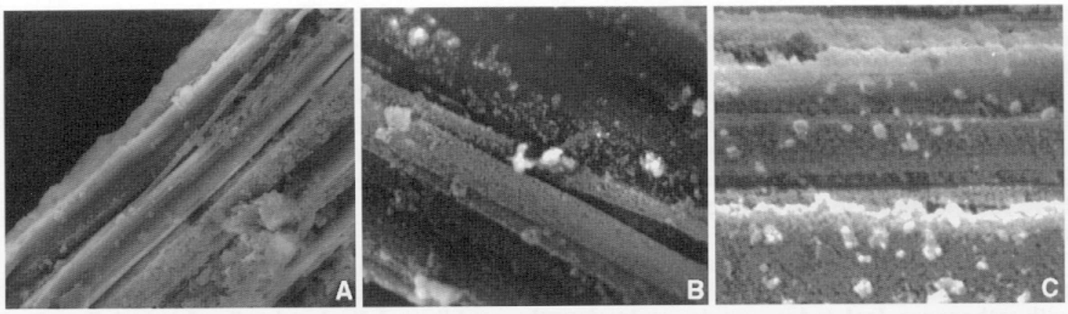

TEXT-FIG. 4. Conodont specimen C721a, Soom Shale, Sandfontein, South Africa; Ordovician (Ashgill). A, smooth muscle fibres *c.* 5 μm in diameter showing longitudinal lineation reflecting myofibrillar structure; × 1200. B, myofibrils showing microgranular texture; × 6300. C, myofibrils showing microgranular texture; × 7500.

material in C679a, seven gave a quartz composition and one gave excitation peaks in Al, Si, S, Cl and Fe, which is problematical, but may represent illite and alunite. The third, and most common mode of preservation of the denticle core prismatic enamel is mouldic (see Text-fig. 3L). The severe apatite dissolution suffered by conodont elements from the Soom Shale can be seen clearly in Text-figure 3L where the denticle should point out of the plane of the photograph. Instead, only a stub representing its former position is seen.

Conodont elements are composed of calcium phosphate in which fluorine substitutes for hydroxides, producing francolite (Pietzner *et al.* 1968). There are three vertebrate hard tissue types that are pertinent to the taphonomy of the conodont elements from the Soom Shale. These are dentine of the basal body, and prismatic and aprismatic enamel of the denticle crowns (Phil Donoghue, pers. comm. 1996). Dentine is an organic-mineral composite in which the apatite crystallites are considerably smaller (average 200–1000 angstroms long, 30 angstroms wide) than those in enamel (1600–10000 angstroms long, 400 angstroms wide) (Carlson 1990). The inorganic component of dentine constitutes approximately 70–75 wt % and the organic component constitutes 18–21 wt % (Carlson 1990). The organic material is largely collagen (Scott and Symons 1977) within which the hydroxyapatite crystallites are more or less randomly orientated (Carlson 1990). In the Soom Shale conodont elements, dentine tissue has been replaced by illite and alunite. Conversely, enamel has non-collagenous organic matter which comprises typically less than 1 wt % of the tissue, and is a highly mineralized tissue with an inorganic component constituting up to 97 wt %. The enamel crystallites may be orientated in different ways. In aprismatic enamel, all crystallites are more-or-less mutually parallel and are perpendicular to the enamel dentine junction. Prismatic enamel shows a repetitive pattern of variation in crystallite orientation producing 'prisms' (Carlson 1990). This tissue type has been most commonly replaced by quartz (and rarely by illite and alunite) in the Soom Shale. In light acid preparations of conodonts, dentine is more sensitive to acid dissolution than aprismatic enamel which is more sensitive than prismatic enamel (Phil Donoghue, pers. comm. 1996).

Theron *et al.* (1990) noted the poor preservation of the original apatite in the elements from the Soom Shale, with several represented by internal or external moulds. On analysis of greenish material by EDX, peaks in silicon, aluminium and potassium were obtained, presumably representing illite from the matrix. Peaks in calcium and phosphorus were obtained from some relatively unaltered amber-coloured areas of one of the ramiform elements (Theron *et al.* 1990, text-fig. 4); this may represent an alunite group mineral. The mode and mineralogy of conodont element preservation in the Soom Shale is unique and its elucidation will require detailed chemical mapping.

Conodont soft tissues. The preserved soft tissues of the trunk myomeres were shown by both EDX

(Table 2A) and electron microprobe analysis (Tables 2B and 3A) to be composed only of illite/mixed layer clay. The muscle blocks, or myomeres, preserve ultrastructural details of the muscle fibres including fibrils and sarcomeres (Gabbott *et al.* 1995). The muscle fibres in the myomeres are *c.* 3–5 μm in diameter and have a circular cross section (Text-fig. 4A). Their preservational textures vary; most fibres are very smooth (Text-fig. 4A) whereas others have a distinct granularity (Text-fig. 4B–C). The smooth fibres are unlike any other fossilized muscle fibres figured from fish or other taxa. The granular texture, where present, usually composes the whole fibre, but it may appear on smooth fibres as a patchy coating. The texture comprises spherical–sub-spherical granules with a diameter of *c.* 90–150 nm. The nature of these microspheres is not yet known because the resolution of the image at the levels of magnification required to view them is very poor. They may be mineralized microbes; fossil nannobacteria have been found as small as 0·1 μm in diameter (Folk 1993). Alternatively, they may be inorganic in origin and analogous to the microspheres/microgranules composed of calcium phosphate recorded in other mineralized muscle tissue (Wilby 1993*a*, 1993*b*).

The sclerotic eye capsules from Keurbos show a similar style of preservation to the chitinozoans from this locality. Some comprise the flattened, black remains of the sclerotized tissues (e.g. C288, C351, C358; see Aldridge and Theron 1993, pl. 1, figs 2–4), whilst others are partially or completely mineralized by a silvery white mineral (C279; see Aldridge and Theron 1993, pl. 1, fig. 1), presumably illite. Often, the part of a specimen preserves the eyes dominantly in black coalified organic material whereas the counterpart is dominantly mineralized. The conodont eye capsules from Sandfontein are composed of a silvery-white mineral which appears the same as the illite/mixed layer clay preserving the somites of specimen C721. These silvery-white patches may be amorphous or have a fibrous texture. The mineralized extrinsic eye musculature has not yet been analysed because specimens are too rare for destructive analysis, and the slabs of shale are too large for the eyes to be positioned under the beam in an SEM chamber. However, the texture, colour and form of the mineral suggest that it is illite/mixed layer clay.

The eye capsules (Aldridge and Theron 1993) of *Promissum pulchrum* are thought to have been composed originally of scleratin, a decay-resistant structural polymer. Decay experiments (Briggs and Kear 1993*a*) on polychaetes have demonstrated the resistance of sclerotized tissue; it was the only tissue type to survive beyond 30 days in the absence of early diagenetic mineralization. Thirty-eight pairs of sclerotic eye capsules have been found from the Soom Shale associated with bedding plane assemblages (eyes occurring with 20–25 per cent. of the conodont apparatuses), whereas only specimen C721 preserves both trunk somites and evidence of eyes, in the form of extrinsic eye musculature. Two additional specimens (C699 and C712) from Sandfontein display very poorly preserved eye musculature but no trunk trace is evident.

Spores and acritarchs. Spores and acritarchs have walls composed of sporopollenin and were recovered following dissolution of the matrix in hydrofluoric acid (Gray *et al.* 1986). These organic-walled microfossils were highly resistant to microbial decay and inorganic degradation. Spores and acritarchs from the Soom Shale are dark brown to black due to considerable thermal alteration and are probably composed of altered sporopollenin. It is possible that some may now be composed of illite but owing to their method of extraction and their small size rendering them invisible on bedding surfaces, this is not testable.

Chitinozoans. EDX analysis on a silver-white chitinozoan from Keurbos gave compositions of illite and illite and alunite, with an iron oxide phase and accessory Cl and Ti (Table 2A). It is not known in which mineral phase(s) the Cl occurs, but Ti probably occurs in illite. Chitinozoans on weathered bedding surfaces from Keurbos are often dark grey/black in colour with a reticulate surface pattern consistent with fractures produced by heating (see Burmann 1969). Other vesicles are preserved in a silvery-white material. Some chitinozoans appear flat whereas others are more three-dimensional; in the latter case, some sediment infill is evident.

EDX analyses on chitinozoans from Sandfontein all gave illitic compositions ± an iron oxide. Ti was recorded in two analyses and Cl in three analyses but these elements did not occur together. At Sandfontein, the chitinozoans are completely mineralized by illite, but again it is unclear whether the mineralization represents an overgrowth or a replacement of the organic wall. The illite crystals on the margin of the vesicle are aligned parallel to it (perpendicular to the bulk of the crystals), whereas the crystals replacing the bulk of the vesicle are aligned approximately parallel to each other and to the long axis of the chitinozoan. These crystals show typical illite habit but are relatively large, being up to 30 μm long, indicating the onset of conversion to muscovite. It is possible that at Sandfontein these are vesicles composed of organic material but they may have been overlooked as the matrix is black.

The original pseudochitinous composition (Traverse 1988) of chitinozoans has been replaced by illitic clay minerals which appear to have formed as a film-like sheet on to the organic surfaces of the vesicles. However, it is not clear whether the organic vesicle survives beneath the clay mineral sheet or has been replaced by it. Soom Shale chitinozoans have been found after HF digestion of the matrix and occur as highly coalified individual vesicles (Cramer *et al.* 1974) or as individuals, chains and clusters on bedding surfaces from Keurbos and Sandfontein. Thus two preservational styles for chitinozoans are distinguishable: organic walled coalified forms found after HF digestion, and those found preserved in clay minerals on bedding surfaces (Table 2A).

Summary of fossil analyses

Table 1 shows the original and fossil compositions of various taxa in the Soom Shale. A summary of the results of EDX analysis is shown in Table 2A and a summary of electron microprobe results in Table 2B. The data clearly split into three compositional groups. One group shows a range of illite mineral group compositions, another group shows a range of compositions in the alunite mineral group, and a third group shows a mixture of illitic and alunitic signatures. This third group is the result of the electron beam overlapping and analysing both minerals. An iron oxide phase was also recorded in a small number of analyses.

No alunite component was recorded from the conodont muscle tissue. The eurypterids, orbiculoids and trematids analysed had both illitic and alunitic mineral signatures. Light microscope, SEM and secondary electron images failed to reveal any distinct pattern to the partitioning of these two minerals. They appear to be intimately mixed.

Illite. Table 3A shows the mean electron microprobe analysis and cation proportions (calculated to 22 oxygens) for the illitic component of the eurypterids, trematids and conodont muscle tissue. It can be seen from the triangular plot (Velde and Meunier 1987; Text-fig. 1A) of the full gamut of analyses that there is some variation in composition, although nearly all samples plot within the illite and mixed-layer clay solid solution series. For simplicity, the fossil compositions which lie in the illite to mixed-layer clay compositional fields will be referred to as illites hereafter because the quantitative electron microprobe analyses demonstrate a continuum of Fe and Mg values from low weight per cent. in purer illites up to 4·08 (Fe) and 2·06 (Mg) in mixed-layer clays.

Alunite. Table 3B shows the mean electron microprobe analyses and cation proportions (calculated to 22 oxygens) for the alunitic component of the eurypterids, trematids and orbiculoids. The compositional field of the alunitic Soom Shale fossils relative to related mineral species is shown on the triangular plot in Text-figure 1B. Note that if more cations, such as Pb, had been analysed for and were present, then fossil compositions would cluster more towards the cation apex. Quantitative electron microprobe analyses show that crandallite ($CaAl_3(PO_4)_2(OH)_5.H_2O$) is the most common alunite group mineral present especially in the orbiculoids; alunite ($KAl_3(SO_4)_2(OH))_6$ also occurs commonly. Calcium constitutes the cation with the greatest weight per cent. in most analyses (19 out of 24), followed by potassium and then iron. A bivariant plot of CaO against P_2O_5 (Text-fig. 5B) for the alunitic fossil compositions shows a positive correlation coefficient (0·41). A

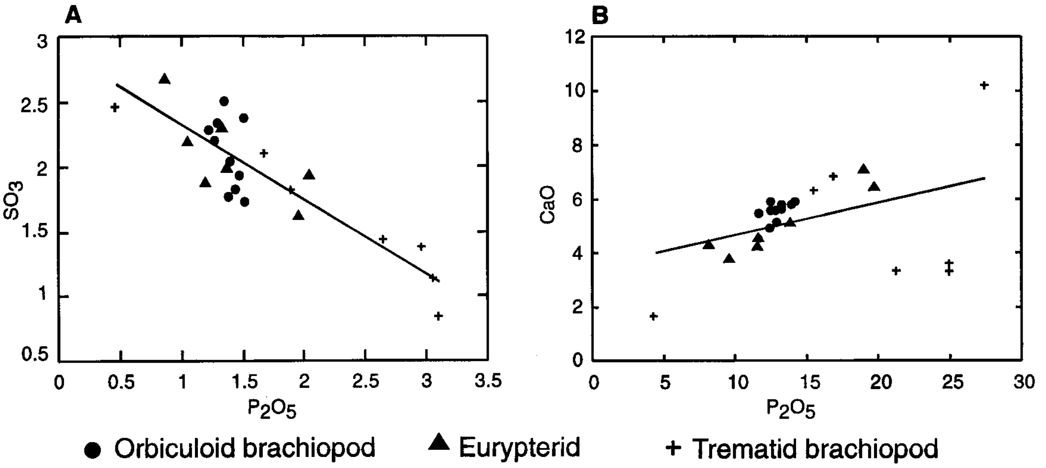

TEXT-FIG. 5. Bivariant plots of fossil material with alunitic compositions analysed by the electron microprobe. A, SO_3 against P_2O_5; there is a strong negative correlation coefficient (R = 0·88) demonstrating extensive anion substitution. B, CaO against P_2O_5 showing a slight positive correlation (R = 0·41) suggesting that both occur, at least quite often, in the same mineral: crandallite.

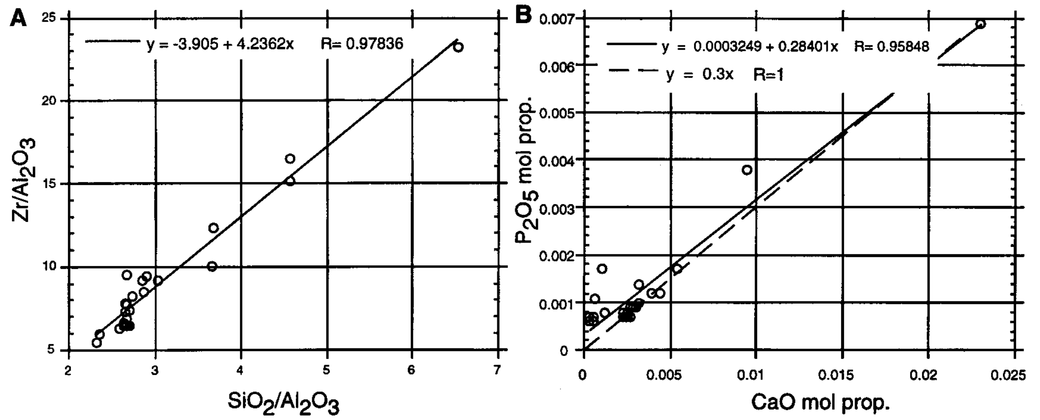

TEXT-FIG. 6. A, alumina normalized bivariant plot of Zr against SiO_2. Zr (ppm.) and SiO_2 (wt %), values from XRF analyses. B, bivariant plot of calculated P_2O_5 (molecular proportion) against CaO (molecular proportion). Stochiometric apatite is represented by the dashed line and has a slope of 0·3; oxide analyses from XRF data.

student *t*-test (n = 24) shows that there is only a one in 20 chance of this correlation coefficient occurring by chance between CaO and P_2O_5. Substitution between the anions P_2O_5 and SO_3 is indicated by their high negative correlation coefficient (Text-fig. 5A).

Discussion of sediment analyses

Mineralogy. The most pristine sediment is from the core material and comprises dominant quartz and illite, together with chlorite, kaolinite, pyrite, and less commonly apatite and alunite. The quartz is probably detrital in origin, as shown by its high correlation coefficient with Zr on an Al_2O_3

normalized plot (Text-fig. 6A, R = 0·98) (see Norry *et al.* 1994). The origin of the illite is more equivocal. It may be detrital or authigenic, formed by the breakdown of K-feldspar (producing mica and/or illite), or both:

$$\underset{\text{K-feldspar}}{3KalSi_3O_8} + 2H^+12H_2O \rightarrow \underset{\text{illite and/or mica}}{KAl_3Si_3O_{10}(OH)_2} + 6H_4SiO_4 + 2K^+ \qquad (1)$$

The breakdown of K-feldspar to form illite and/or mica yields excess potassium (equation 1) which may be used to form additional illite. K-feldspar becomes unstable as pore water acidity increases [as$(K^+)/(H^+)$ decreases], so that breakdown is most likely to have occurred during early diagenesis when organic decomposition by sulphate reducing bacteria produced H_2S ions (equation 2).

$$18CH_2O + 9SO_4{}^{2-} \rightarrow 18HCO^{3-} + 9H_2S \qquad (2)$$

No K-feldspars have been observed in the Soom Shale, either by XRD or SEM, indicating that if illite was formed from their breakdown, this process was very active and complete. The X-ray data indicate that the illite is the $2M_1$ polytype. After changing to mica (equation 1), the K-feldspars may alter to kaolinite (equation 3) (Krauskopf 1982) as porewater acidity increased as a result of organic matter decomposition.

$$\underset{\text{mica}}{KAl_3Si_3O_{10}(OH)_2} + H^+ + 3H_2O \rightarrow \underset{\text{kaolinite}}{3Al_2Si_2O_5(OH)_4} + K^+ \qquad (3)$$

The presence of kaolinite in the core samples is shown by fairly sharp peaks in diffractometer traces but was not detected by electron microprobe analyses. This is probably due to beam overlap, with illite swamping the kaolinite signature. Small amounts of kaolinite may also have formed during the deep arid weathering.

The composition of chlorites in core samples (Table 4 and Text-fig. 1) is consistent with them being clinochlore-chamosite chlorites with approximately equal amounts of Fe and Mg on an atomic basis (Bayliss 1975; Bailey 1988). There is no excess Al, so that the analyses fall into the normal range for chlorites formed by metamorphism rather than in the diagenetic range (Velde and Meunier 1987). This is a slightly higher temperature than that estimated for the Soom Shale (200 °C) from the colour of palynomorphs (Cramer *et al.* 1974; Gray *et al.* 1986). In addition, some chlorites of clinochore-chamosite composition may have been derived and therefore introduced detritally into the Soom Shale sediment.

Apatite was detected, by electron microprobe analysis, in one of the more silty core samples. XRD analysis failed to find any further apatite in any core samples so it is either rare or amorphous. A bivariant plot of the calculated molecular proportions for CaO against P_2O_5 demonstrates an excellent positive correlation coefficient (R = 0·96), a near zero intercept and a slope of 0·284, which is very close to the slope value of 0·3 that would apply if all the calcium and phosphorus were situated in apatite (Text-fig. 6B). This indicates that the sediment is extremely calcium carbonate deficient.

Finely disseminated pyrite occurs in most of the core samples; it is of diagenetic and syngenetic origin and will be discussed later under the heading DOP (degree of pyritization).

A single XRD trace (out of the 35 samples) from core sample K1.2 indicated the presence of alunite, the formation of which is discussed later.

Sediment from Keurbos consists of quartz, illite ($2M_1$ polytype), chlorite, kaolinite and anatase (detected by XRD analyses). With the exception of the presence of kaolinite and the absence of alunite, this is the same mineralogy as at Sandfontein. The absence of sedimentary alunite from Keurbos again indicates that it is an extremely rare component of the matrix, although fossil material from Keurbos always contains some alunite (Table 2A–B).

Samples from Sandfontein contain quartz, illite, anatase, possible chlorite and, in one sample only (KS4A), alunite (detected by electron microprobe and XRD analyses). Again, the illite is of the $2M_1$ polytype and constitutes the largest component of the sediment. The absence of kaolinite in samples from Sandfontein remains to be explained, as it is present in the core samples and heavily

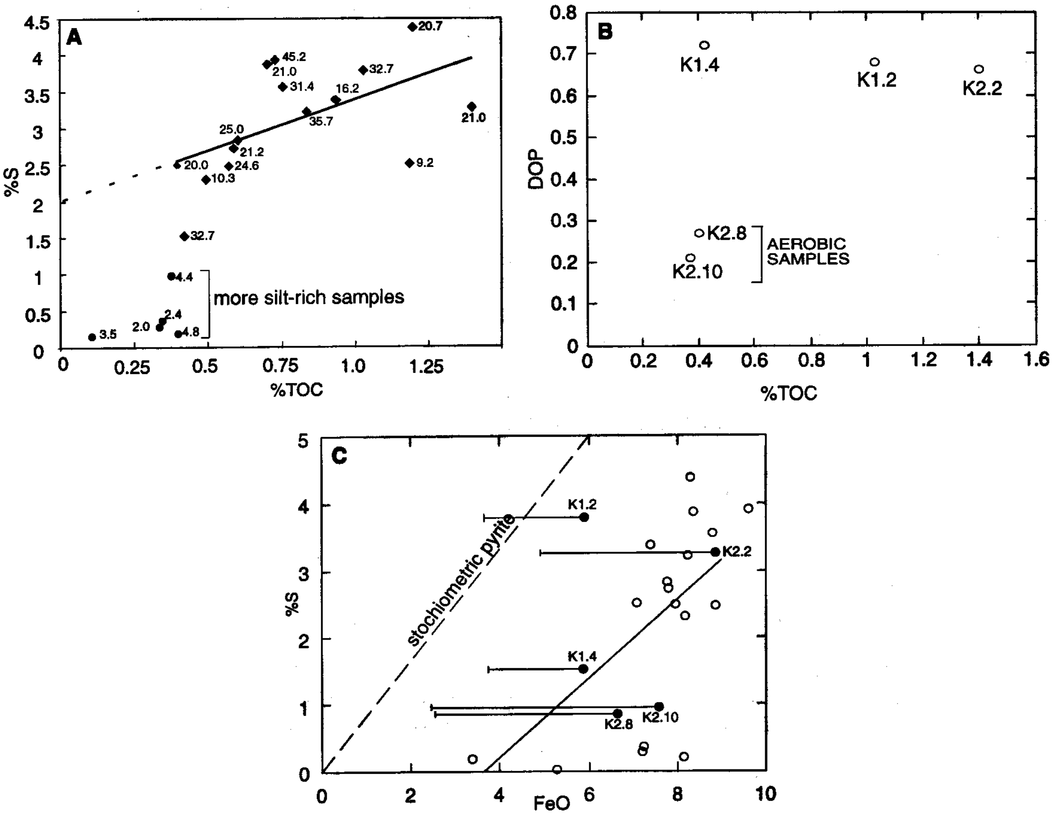

TEXT-FIG. 7. A, bivariant plot of % S against TOC (total organic carbon wt %) for unweathered core samples. Diamonds represent samples with high Mo contents (indicated in ppm.); circles represent samples with low Mo contents (indicated in ppm.). For samples with high Mo, % TOC and % S, R = 0·31. B, bivariant plot of DOP (degree of pyritization) against TOC for five core samples. C, bivariant plot of % S against FeO wt % for unweathered samples. Solid circles denote samples on which DOP has been analysed and the solid lines to the left of each sample represent the amount of acid soluble iron extracted from each sample in wt %. The dashed line represents calculated stochiometric pyrite. Note that for sample K1.2 pyrite becomes soluble during iron extraction. $y + -2{\cdot}1379 + 0{\cdot}58507x$; $R = 0{\cdot}56982$.

weathered samples from Keurbos. Although only two samples from Sandfontein (K3.1 and K3.2) have been analysed by X-ray diffraction, kaolinite was also not detected by electron microprobe analysis. Chlorite was absent in the two XRD analyses, but electron microprobe analyses show a probable mix of illite and chlorite in KS4A from Sandfontein. The sources of the illite and chlorite are probably the same as discussed for the core sample sediments, but the origin of the anatase is unclear. It is commonly a detrital mineral in sedimentary rocks, but may be authigenic or produced by low temperature hydrothermal fluids. Its absence from fresh core material, however, indicates that the anatase in the Soom Shale is probably the result of a near surface, weathering process.

The electron microprobe analyses of alunite grains show that FeO is the most abundant cation, with roughly equal amounts of CaO and K_2O and smaller, but significant amounts of Ce_2O_3, La_2O_3 and SrO. Of the anions, P_2O_5 is only slightly higher in abundance than SO_3 (Table 4; Text-fig. 1B) and any single end-member alunite group mineral is not distinguishable; this is unlike the fossil alunites where end member minerals are clearly distinguished. Viewed optically and under secondary electrons, the alunitic grains (three analysed in total) are rounded with a discontinuous halo and all are very poorly preserved. The grains of alunite found within the sediment may have been associated with a fossil fragment. Alternatively, alunite may form a rare but authigenic component of the sediment. In any case, alunite group minerals are an extremely uncommon component of the matrix with only three grains being found in polished thin sections. Unlike the sedimentary alunite analyses, those from fossil material commonly show SO_3 and P_2O_5 substitution as demonstrated by their good negative correlation coefficient ($R = 0{\cdot}88$, Text-fig. 5A). Their possible genesis is discussed later.

Molybdenum. The molybdenum concentration in unweathered core samples, with no significant silty component, is 9·20–45·20 ppm. (average = 24·46 ppm.), considerably higher than in PAAS (Post Archean Average Shale; 1·0–2·0 ppm., Taylor and McLennan 1985). Molybdenum enrichment in black shales has been documented by several workers (e.g. see Brumsack 1989). Helz *et al.* (1996) have shown using EXAFS (extended X-ray absorption fine structure) spectra that molybdenum, a conservative element in normal marine waters, becomes particle reactive when the action point of HS^- reaches $10^{-3{\cdot}6}$–$10^{-4{\cdot}3}$; hence HS^- acts as a geochemical switch. When *a*HS^- approaches this value Mo may form covalent bonds, via S bridges, with sedimenting particles containing transition metals (e.g. Fe) and organic molecules; in this way, Mo is scavenged from the water column and incorporated into the sediment (Helz *et al.* 1996). Since HS^- concentrations in natural anaerobic waters range to values above 10^{-3} M, the *a*HS^- switch will be activated in many such environments (Helz *et al.* 1996). The elevated Mo content in the Soom Shale sediment, therefore, strongly suggests that anoxic conditions prevailed. Where low Mo concentrations are recorded in unweathered samples, these are invariably from more silt-rich rock (see Text-fig. 7A).

Total organic carbon, total sulphur and degree of pyritization (DOP). Table 6 shows the results of total organic carbon, % sulphur and DOP analyses. In unweathered samples and samples with no silty laminations, the TOC ranges from 0·11–1·4 wt % and S ranges from 0·2–4·38 wt %. A plot of % S/TOC (Text-fig. 7A) for unweathered Soom Shale shows two distinct data groupings which are well defined by their Mo contents. Samples with high Mo contents (9·20–45·20 ppm.) show a positive correlation with a positive intercept on the y axis (y = 2·0). Samples with low Mo, % S and TOC values occur towards the top of the Soom Shale, where coarser silty laminations are common. C/S ratios are listed in Table 6, and all the unweathered samples plotted (Text-fig. 7A) range between 0·16–1·95. In euxinic conditions, C/S ratios are consistently less than 3 and regression lines with positive intercepts on the S axis have been demonstrated (Berner and Raiswell 1983; Levental 1983), but it is important to note that some of the organic C may have been lost during anchimetamorphism.

During the deposition of the Soom Shale, bottom and pore waters became rapidly aggressive towards aragonite and calcite resulting in their complete dissolution. Apatite was also dissolved, but at greater burial depths than the carbonate phases. Corrosive fluids could have been produced by the build-up of H_2S and H^+ in solution as a result of active sulphate reduction, where there was a paucity of reactive iron. Thermal maturation probably accounts for the relatively low TOC content and may have remobilized sulphur and iron phases so that caution is necessary when interpreting the results of these analyses.

In normal marine environments, with oxygenated bottom waters containing adequate reactive iron, the principal factor limiting pyrite formation is the amount of buried organic matter. However, in euxinic environments, H_2S is present above the sediment-water interface as well as within the sediments. Consequently, pyrite can form before burial in the presence of sedimenting minerals containing reactive iron. In this situation, it is not organic carbon that limits the production of pyrite, owing to the omnipresence of H_2S, but the amount of reactive iron in the sediment (Raiswell 1982; Berner 1984; Fisher and Hudson 1985). Reactive iron may be defined as the fraction of iron in marine sediments which readily reacts with sulphide (a product of sulphate reduction) to form iron sulphide minerals and eventually pyrite (e.g. Berner 1970; Raiswell and Berner 1985; Canfield 1989). The two most important sources of reactive iron in fine-grained sediments are probably iron oxides (Canfield 1989) and colloidal ferric oxides adsorbed on to clay minerals (Berner and Rao 1994). Canfield (1989) has shown that there was a complete consumption of iron oxides at the FOAM (Friends Of Anoxic Muds) site at Long Island Sound, USA, by 70–100 mm depth. The FOAM site sediment is anoxic and Fe-poor and early pyrite appears to form at the expense of iron oxides (e.g. ferrihydrite, lepidocrocite, goethite and hematite) with no evidence for substantial involvement of iron silicates (Canfield 1989). At this locality, reoxidation of pyrite due to bioturbation and other processes (e.g. wave action) constantly replenishes iron oxides, without which the sediment would have become considerably more 'sulphidic' (Canfield 1989). The reactivity of iron adsorbed on to clay minerals towards H_2S has not been studied in any detail.

In sediments of Devonian to Cretaceous ages, the DOP may give a fair indication of the degree of bottom water oxygenation (Raiswell *et al.* 1987). However, pre-Devonian sediments would have had relatively more reactive organic carbon material (due to the absence of terrestrial plant-derived organic matter) and would therefore produce more sulphur fixation (as pyrite) per unit of buried carbon (Raiswell and Berner 1986). To date, then, the use of DOP as an indicator of bottom water oxygenation in pre-Devonian sediments is not secure, but it can be used to gauge the amount of iron reactive towards H_2S. The amount of reactive iron would have been important in controlling the pH of the pore waters in the Soom Shale sediment. For example, sufficient quantities of reactive iron oxides (and ferric oxides sorbed onto clay minerals) could have effectively buffered the concentration of pore water sulphide to very low levels, even in the presence of active sulphate reduction.

The five samples analysed for DOP from the Soom Shale fall into two groups (Table 6), one with moderately high DOP values (0·72, 0·68 and 0·66) and another with low DOP values (0·21 and 0·27). The samples with low DOP values also have low Mo, % S and TOC (Text-fig. 7A), are more silt-rich and occur towards the top of the Soom Shale. A plot of DOP against TOC (Text-fig. 7B) shows that there is no correlation between the amount of organic carbon and the DOP in the three samples with high DOP values. In this situation, the amount of detrital iron minerals reactive towards H_2S is the limiting factor in pyrite formation rather than the amount of organic carbon. In this case, the plot of % S against % TOC (Text-fig. 7A), demonstrating a positive correlation, indicates that there was more Fe available for increased levels of syngenetic pyrite formation at higher C values (Raiswell and Berner 1985). Thus, at least at times when the bottom waters were O_2-depleted, it would appear that pyrite formation was syngenetic and limited by the amount of reactive iron. However, this is in contradiction with the DOP values, which are not excessively high, and with the amount of acid soluble iron (Table 6 and Text-fig. 7C) which would have been available for pyrite formation. There are two possible and related explanations to account for the discrepancy between demineralized carbonate phases and moderate DOP values; one involves experimental error in the determination of acid-soluble iron which should have been reactive towards H_2S.

The plot of % S against FeO (Text-fig. 7C) shows the amount of acid soluble iron determined after boiling in HCl for the five samples on which DOP was analysed (represented as solid horizontal lines). In sample K1.2 (DOP = 0·68), some of the pyrite iron became soluble through boiling in HCl. This obviously places some doubt on the accuracy of the amount of acid soluble Fe determined in the other samples. Furthermore, the amount of acid soluble iron determined may have been further enhanced by Fe from chlorite and illite. In an examination of iron extraction techniques for the determination of DOP, Raiswell *et al.* (1994) found that during boiling in HCl (the technique used here) some iron was released from silicate phases, particularly nontronite (7·13 ± 0·36 wt %) and chlorite (2·19 ± 0·11 wt %) that would not have been reactive towards H_2S. In the Soom Shale, Fe contained within silicate phases may have come from chlorite (mean Fe wt % = 23·58; see Table 4 for electron microprobe analysis) and illite (mean Fe wt % = 1·66, see Table 4). Therefore, experimentally determined values of acid soluble Fe may be higher than the amount of Fe that would have actually been available to react with H_2S during early diagenesis. Thus syngenetic pyrite formation may have exhausted all or most of the detrital iron so that diagenetic pyrite formation did not occur or at least was very slow.

Another explanation may be that there was a paucity of iron oxides available for reaction with the H_2S produced by sulphate reduction. It may be that pyrite formation was initially inhibited, by a lack of reactive iron oxides, allowing increased bottom/pore water acidity, and could only commence when pore waters became aggressive towards iron-containing silicate minerals and released iron from them. In addition, there would have been no recycling of iron by bioturbation or wave activity. A paucity of iron oxide minerals in the Soom Shale is corroborated by XRD and EM analyses of the sediment and may be explained by an iron oxide-poor sedimentary source to the basin. Furthermore, sediments at this time would not have supported a soil horizon in the absence of land plants and the land surface had presumably been scraped clean by ice.

SOFT TISSUE PRESERVATION

Soft tissues, such as muscle, are subject to rapid autolysis and metabolization by bacteria. They are lost very rapidly unless preserved by early authigenic mineralization (Allison 1988*a*, 1988*b*, 1988*c*; Briggs and Kear 1993*b*, 1994). In the fossil record, examples of authigenic minerals which replace soft tissues are phosphate (e.g. Müller and Walossek 1985; Martill, 1988, 1990), and more rarely and with less fidelity, pyrite (e.g. Stürmer 1970; Cisne 1973; Conway Morris 1986; Briggs *et al.* 1991*a*; Briggs *et al.* 1996; Wilby *et al.* 1996) and carbonate (Wuttke 1983). Silicification of soft tissues is known only from one example, the Eocene lignite of Geiseltal (Voigt 1988).

In the Soom Shale, soft tissues are replicated by clay minerals (conodont muscle tissue) and by clay minerals and alunite group minerals (eurypterid cuticle and muscle tissue); these minerals have hitherto not been recorded preserving soft tissues in the fossil record. The fidelity of replication is at a sub-cellular scale, a level of detail which has only previously been reported in soft tissues replaced by phosphate (e.g. Martill 1990; Wilby 1993*a*, 1993*b*). Any model proposed to explain the preservation of extremely labile tissues by clay minerals must also account for the mode of preservation of more recalcitrant organic molecules such as chitin (eurypterid and naraoiid exoskeleton), pseudochitin (chitinozoan vesicles) and scleratin (conodont eye capsules). All of these organics have been partly or wholly replaced, or surface coated, by clay minerals. Only the inert organic compound sporopollenin, which makes up the walls of acritarch and spore palynomorphs seems unaffected by the mineralization event(s) that affected most other biomolecules. It is possible that bacterial mediation is a requirement, and some bacterial decay is necessary before mineralization of organic substrates can occur (Wilby 1993*a*, 1993*b*). In addition, replication of biomolecules by any mineral may require some prior decay of the substrate so that charged broken bonds become available as potential nucleation sites. The fidelity of replication of scleratin, pseudochitin and chitin is not as high as in the labile muscle tissue. Indeed, only the gross morphology of structures composed of scleratin and pseudochitin is preserved. Thus, the variation in biomolecule preservation (presence or absence as altered coalified organics, mineralized films or mineralized replacements) is probably most strongly influenced by their relative resistance to decay and thermal degradation. In addition, the fluctuation of ambient bottom and pore water conditions would have affected the mode of preservation. For example, the variation in the preservation of chitinozoan vesicles demonstrates that the conditions necessary for the mineral replacement and/or overgrowth were not always prevalent during early diagenesis. The mode of preservation of phosphatic fossils with an integral organic component, such as the conodont elements and lingulate brachiopods, must also be considered.

The evidence strongly suggests that the soft tissues of organisms in the Soom Shale were replaced directly by clay minerals. The sub-cellular fidelity of replication is difficult to reconcile with more than one stage of mineralization. In addition, the geochemical environment at the time of deposition would have aided clay mineral/organic interactions whilst militating against phosphate, pyrite or carbonate interactions with the organic material. However, the involvement of a phosphate precursor phase has been demonstrated in a number of cases (e.g. Allison 1988*b*; Martill 1988; Wilby 1993*b*) and should not be dismissed without further consideration here.

Two stage replacement model

The possibility of a carbonate or pyrite precursor to the replacive clay minerals is not considered tenable, given the acidic nature of the bottom waters and the demonstrated paucity of reactive iron oxide minerals. Authigenic mineralization of soft tissues by calcium phosphate has, however, been shown to occur commonly and extremely rapidly (Martill and Harper 1990; Briggs and Kear 1993*b*, 1994). Chitin is known to be phosphatized in arthropods from the Orsten and the Alum Shale (Upper Cambrian, Sweden), where preservation of soft integument and cuticular structures may have occurred as either a coating or complete replacement (Müller 1985). However, there are no examples yet known of phosphatized chitinozoans, and tissues originally composed of scleratin have not been reported as phosphatized replacements.

One example of soft tissues having been phosphatized and subsequently replaced by other minerals comes from the marine Jurassic biota of La Voulte (Wilby *et al.* 1996). Here, three-dimensional soft-bodied animals and their internal organs are preserved in an unusual suite of minerals with a consistent diagenetic sequence (apatite → calcite ± gypsum → pyrite ± chalcopyrite → galena) (Wilby *et al.* 1996). This is believed to show the importance of apatite as a 'template' for calcification and pyritization in soft tissue preservation (Wilby *et al.* 1996). With each mineral transformation, a loss in the fidelity of soft tissue replication occurred, so that the apatite shows details of muscle fibres, whereas replacement calcite preserves gross morphology only. The calcite phase not only replaced apatite but also filled voids between and within soft tissues, while the pyrite coated previously phosphatized, thick (white) muscle fibres of crustaceans and replaced their calcified thin (red) muscle fibres (Wilby *et al.* 1996). Although the La Voulte deposit appears to be singular in its preserving mineral suite, it does demonstrate that replacement of phosphate by other minerals is possible.

However, a number of lines of evidence militates against precursive phosphatization of either labile or recalcitrant biomolecules in the Soom Shale: (1) the geochemical environment in the Soom Shale was not conducive to phosphate concentration and precipitation; (2) no traces of calcium or phosphorus have been detected in the conodont or eurypertid muscle tissue from EDX or electron microprobe analyses, signifying that clay minerals have entirely replaced phosphatized muscle tissue and have not simply coated an earlier phosphate phase; (3) no clay minerals have been found replacing the crown tissue in conodont elements, so crystalline apatite was not replaced by clays; and (4) the clay minerals preserve sub-cellular details indicating that they were not a later void fill.

The myomeres of the conodont animal are extensively mineralized but there is no evidence to suggest that conodonts contained large quantities of phosphate. Hence, concentration of phosphate within the sediment, either on to mineral surfaces or into bacteria, would have been a prerequisite for such extensive phosphatization. However, the anoxic condition of the sediment, even on the sea floor, would have prohibited any concentration of phosphorus by adsorbtion on to ferric oxides/hydroxides and clay minerals (see Ingall *et al.* 1993). In addition, the storage and release of phosphorus by bacteria is redox-dependent, and uptake and storage of phosphorus is favoured under aerobic conditions where excess phosphorus is available (Gächter and Meyer 1993). Therefore, it is unlikely that any phosphorus liberated from organic matter decomposition would have been extensively incorporated into bacteria in the anaerobic Soom Shale sediment. It seems arguable that the anoxic sediment and bottom waters could not have concentrated sufficient phosphorus to phosphatize soft tissues.

For replacement of an initial phosphate phase by clay minerals, geochemical conditions would have been required in which the pore waters entering the carcass were aggressive towards apatite and simultaneously precipitated clay minerals, or contained clays as a colloidal component capable of replacing the phosphate crystallite by crystallite. That dissolution of calcium phosphate has occurred in the Soom Shale is demonstrated by the mouldic preservation of lingulate brachiopods and conodont elements; this would have required the presence of large quantities of acidic waters. Kaolinite can precipitate authigenically from acidic waters so acidic conditions suitable for the dissolution of calcium phosphate do not prohibit authigenesis of kaolinite nor, indeed, the presence of colloidal clay minerals. Thus, during calcium phosphate dissolution, clay minerals may have been able to replace apatite almost instantaneously.

The relative timing of any clay mineral replacement of phosphate is hard to constrain. The dissolution of apatite from the conodont elements probably could not have occurred post-lithification as fluid would not have flowed easily through the rock. Dissolution by Recent weathering is also unlikely because it affects the conodont elements from both Keurbos and the less-weathered Sandfontein. A further test of the effects of weathering would be examination of phosphatic fossils from fresh core material to see if they are also mouldic. However, the presence of silica replacements of apatitic conodont material from Sandfontein provides strong evidence: it is difficult to envisage corrosive meteoric fluids capable of dissolving phosphate and of concomitant silica precipitation to be present during weathering. Furthermore, if apatite dissolution occurred during weathering it would be more likely for the replacement clays and silica to be void-filling rather than being high fidelity replacements of the apatite.

The muscle tissue in the conodont animal from the Soom Shale shows good sub-cellular detail (Gabbott *et al.* 1995). By comparison with the La Voulte fossils, this is difficult to reconcile with there having been two stages of replacement. However, colloidal clay minerals are extremely small (1 μm–1 nm in diameter) and it is possible that they could coat on to and replace an apatite precursor without as much information loss as in the calcite and pyrite in the La Voulte deposit. Unfortunately, the morphology of the clay minerals cannot be seen under the SEM because the crystallites are too small. As yet no TEM sections have been made of the conodont muscle tissue but this technique may enable the crystallites to be resolved.

If one mineral phase completely replaces another, it may be extremely difficult to determine whether the initial mineral was ever present unless its crystal habit is pseudomorphed. Lucas and Prévôt (1981, 1984) have reported the transformation of biomineralized carbonate materials into apatite where the original crystal form of the carbonate is conserved. If clay minerals have replaced an initial phosphate phase, then the habit of the apatite crystallites in microspherulitic and microgranular textures may be pseudomorphed. Ideally, microtomed sections of the Soom Shale soft tissues suitable for TEM studies should be made in order to check the crystal habit of the clay minerals for the presence of pseudomorphs. However, the presence of microspherulitic or microgranular textures would not indicate unequivocally the former presence of apatite as other minerals precipitate with this habit. For example, framboidal pyrite consists of discrete equigranular pyrite microcrysts (usually 5 μm in diameter) which can be packed with varying degrees of ordering into nearly spherical aggregates (usually 500 μm) (Canfield and Raiswell 1991, p. 342). Although pyritic framboids are approximately five times the size of apatite microspheres, they demonstrate that microspherulitic aggregates are not exclusive to apatite crystallites.

There is, overall, little evidence to sustain a two-stage phosphate precursor–clay mineral replacement model. The sea floor conditions at the time of deposition of the Soom Shale seem to have been inimical for phosphate concentration, and the high fidelity of muscle replication militates against two phases of replacement.

Direct clay mineral replacement model

Illite and kaolinite may both have been involved in the original replication of soft tissues in the Soom Shale biota, and may also have precipitated on to templates provided by the more recalcitrant chitin, pseudochitin and scleratin. Subsequently, complete replacement of chitin and some pseudochitin occurred but most scleratin was just coated with a thin veneer of clay minerals. Clay minerals at the periphery of the chitinozoan vesicle walls have a mutually parallel orientation different from the random orientation of matrix clay minerals. This supports the hypothesis that the organic matrix acted as a template for the clays. It is possible that scleratin did not promote complete replacement by clays because it did not decay sufficiently for clays to penetrate and nucleate beyond the surface. Alternatively, the chitin and pseudochitin may also have been coated with the organics lost during later diagenesis. This is not supported by the existence of organic chitinozoans in standard palynological preparations, attesting to the ability of pseudochitin to survive the burial temperatures reached in the Soom Shale (Cramer *et al.* 1974).

In the model developed here, kaolinite is considered as the principal clay mineral initially responsible for mineralizing the biomolecules. There is no evidence as yet to suggest that illite could not have formed in the same way, but more is known about the interactions of kaolinite with microorganisms and organic substrates (e.g. Skujins *et al.* 1974; Burns 1979; Theng 1979; Stotzky 1980; Avnimelech *et al.* 1982; Barker and Hurst 1985), and the acidic conditions in the sediment bottom/pore waters would have favoured kaolinite authigenesis.

Colloidal clay particles are well known for their affinity for organic substrates in the presence of cations (Avnimelech *et al.* 1982). A practical use of this has been the clarification of algal blooms in polluted lakes by kaolinite (Avnimelech *et al.* 1982; Ferris *et al.* 1987). This affinity coupled with the small particle size (1 nm–1 μm) of colloidal clays offers the potential for high fidelity soft tissue replication. A model to account for the preservation of soft tissues by clay minerals in the Soom Shale must explain (1) the speed of the reaction, (2) the exclusion of other mineral phases, and (3) why clay mineral preservation appears to be so rare elsewhere.

Kaolinite and/or illite may have been detrital components of the Soom Shale and some probably existed as colloids. Kaolinite could also have grown authigenically in the slightly acidic bottom waters of the basin. MacKenzie and Garrels (1966) proposed that authigenic clay minerals could form rapidly, on a time scale of hours to days, upon contact of detrital clay minerals with seawater. This has been corroborated by Mackin and Aller (1984) based upon dissolved Al distributions from nearshore, low pH sediments of the East China Sea. It has been suggested that Al-Si-H^+ relations are affected by pH, and most authigenesis of mineral phases involving these species occurs under low pH conditions (Mackin and Aller 1984). Moreover, in a low pH environment, a more H^+-rich or cation depleted phase may have been favoured, and would compose the majority of the authigenic material (Mackin and Aller 1984). In their study, Mackin and Aller (1984) showed that dioctahedral chlorites formed authigenically. It is tentatively suggested, therefore, that if clay authigenesis occurred in the Soom Shale under low pH conditions, it was kaolinite, which is extremely depleted in cations, that may have been formed.

The preservation of soft tissues by clay minerals would have been dependent on the properties of the muscle tissue and cuticular cells, especially the charge on the cell membranes. In the aqueous environment, the cell membrane, if similar to that of Recent cells, would have existed as a continuum of lipid and protein organized as a molecular double layer, with the hydrophobic portions of the lipid molecules being opposed and the hydrophilic groups projecting outwards into the aqueous phase (Fletcher *et al.* 1980). The charge of Recent organic cells is dependent upon ionic changes determined by the isoelectric point (pI) or dissociation constant (pK) of exposed functional groups and the pH of the environment (Burns 1979; Theng 1979); it is not known, however, what, if any, effect the death of the cell would have upon the charge. At physiological pH in aqueous environments, most organic substances will have a negative charge with compensatory DDL (diffuse double layer) (Theng 1979; Stotzky 1980); this is presumed to have been the case for the organic substrates of the preserved soft tissues from the Soom Shale.

Detrital kaolinite or illite, or authigenic, colloidal kaolinite and the organic substrate would probably have had net negative charges under the low pH conditions, i.e. a pH that was above the isoelectric point (pI) or the dissociation constant (pK) for both the participants. A prelude to any interaction between the kaolinite/illite and the organic substrate must have been a sufficient reduction in the electrokinetic potentials (EKP) of the participants so that they were able to get close enough to each other for attractive forces, either chemical or physical, to overcome electrostatic repulsion (Stotzky 1980, p. 231). Kaolinite/illite may have become sorbed on to organic surfaces in the presence of an electrolyte; in the marine Soom Shale basin, cations such as Na^+ and Ca^{2+} would have been in abundance. In addition, upon death, cell membranes would have become highly permeable to Ca^{2+} which would have been released and available as an electrolyte (Rob Hirst, pers. comm. 1996). Some investigators have suggested that polyvalent cations are necessary to reduce the electrostatic repulsion through forming complex bridges between the two negatively charged

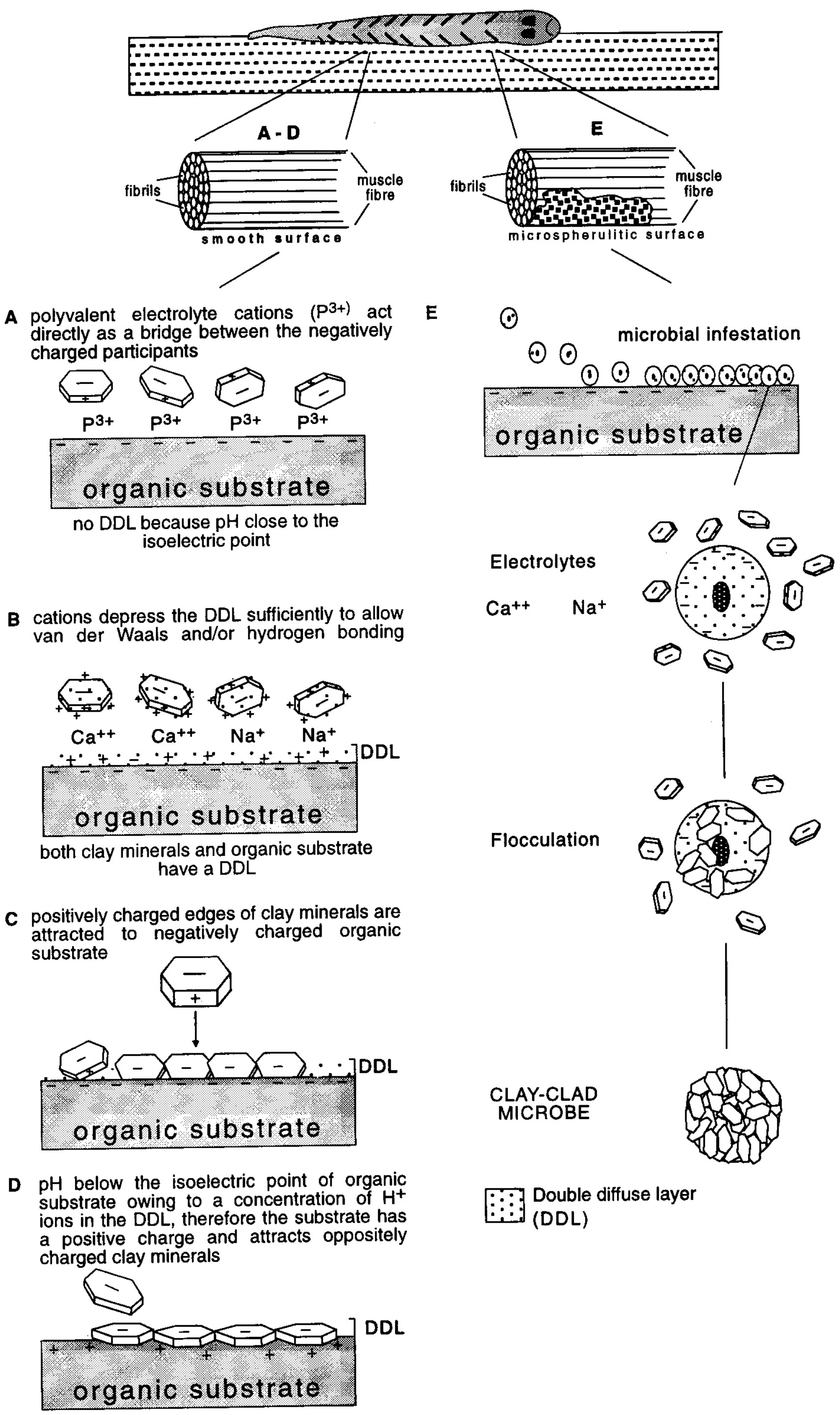

TEXT-FIG. 8. Idealized cartoons to show the possible interaction between clay minerals and organic substrates (A–D), and clay minerals, microbes and organic substrates (E) to replicate soft tissues directly by clay minerals. DDL = diffuse double layer.

participants (Santoro and Stotzky 1967) (Text-fig. 8A). Theng (1979) and Burns (1980) have shown that monovalent cations, by depression of the DDL, may have enabled clay minerals to approach the organic substrate closely enough to bond, by van der Waals and/or hydrogen bonding (Text-fig. 8B). Alternatively, the two participants may have been effectively oppositely charged. For example, the positively charged edges of the clay mineral may have been attracted to the negatively charged organic substrate (Text-fig. 8C). Another possibility is that a localized acidic environment may have been produced by the inclusion of H^+ ions (prevalent in the bottom/pore waters) into the DDL of one of the participants (McLaren and Skujins 1968; Stotzky 1980). As a result, the participants may not have been like-charged (i.e. the pH could have been below the isoelectric point of one of the participants thereby imparting a net positive charge) (Burns 1980). This is shown in Text-figure 8D where H^+ ions have become concentrated in the DDL of the organic substrate thus lowering the pH sufficiently to induce a net positive charge on the substrate because the pH is less than its isoelectric point. The net negatively charged clay minerals would have subsequently been attracted to and adsorbed on to the organic substrate. Thus, it is possible for colloidal clays to be attracted to and adsorbed on to organic substrates either through the presence of electrolytes neutralizing the electrostatic repulsion or by the participants having had opposite charges.

Recently, labile organic matter in marine sediments has been shown to be stabilized by sorption on to mineral surfaces (Mayer 1993; Keil *et al.* 1994); essentially the same process may have occurred in the Soom Shale, but in an opposite direction to that proposed by Mayer (1993) and Keil *et al.* (1994). There is no reason to believe that adsorption can operate only in one direction, i.e. that clays (or mineral surfaces) are always the adsorbates and organics the adsorbents (Stotzky 1980).

Colloidal clay minerals could have nucleated by flocculation and subsequent adsorption on to specific organic substrate templates so that the structural proteins of the conodont muscle tissue were replicated at sub-cellular levels. This specificity is presumed to be related to the abundance and nature of nucleating sites on the template molecule, and indeed, such template specificity has been noted for phosphatized soft tissues (Wilby 1993*b*); quite what control such molecules exert over clay mineral authigenesis is unclear.

Flocculation and adsorption of colloidal clay minerals would have continued until all available nucleating sites were occupied. However, kaolinite authigenesis may have continued, resulting in further mineralization of the soft tissue by accretion of additional crystallites on to the pre-mineralized substrate. Flocculation and adsorption of clay minerals may have terminated when all available organic matter had been bacterially reworked and/or when Eh-pH conditions exceeded those of the stability field for the minerals involved. The latter was possibly initiated by the breakdown of proteins to produce ammonia and consequently a local alkaline environment (Berner 1981). It is not yet understood how surface coating of organic tissues by clay minerals produced three-dimensionally preserved muscle tissues. This is, however, also a problem when phosphatizing soft tissues.

Direct and co-ordinated precipitation of colloidal clay mineral platelets on to organic substrates is consistent with the very smooth appearance of the mineralized muscle tissue in the conodont animal and the eurypterid cuticle. However, in some places on the conodont muscle tissue the surface is composed of small spheres of clay (90–150 nm in diameter) reminiscent of the microspherulitic and micrograular texture reported in phosphatized soft tissues (Wilby 1993*a*, 1993*b*). This does not necessarily mean that there was a precursive phosphate phase of replication; such microspheres may represent bacterial bodies/cells which were subsequently preserved in clay minerals. Prokaryotes actively involved in the breakdown of dead organisms can become autolithified as the tissues they are invading become authigenically mineralized (Wuttke 1983). Fossil bacteria in association with soft tissues have been reported as being preserved in a number of inorganic mineral phases including calcium phosphate (Martill 1988; Willems and Wuttke 1987), silica (Voigt 1988), siderite (Wuttke 1983) and clay minerals (Barker and Hurst 1985). In the Soom Shale, infesting microorganisms may have adsorbed colloidal clay minerals in the same way as organic substrates (see Text-fig. 8A–E). In addition, bacteria have been shown to have a greater flocculating tendency in declining growth or death phases (Harris and Mitchell 1973). In this way, certain portions of the conodont muscle tissue would have become covered with microspheres (see Text-fig. 8E); it would not be expected that autolithified microorganisms could preserve the detail of the soft tissues with the degree of fidelity produced by direct nucleation of clay minerals on to the organic substrate. This, however, will remain untested until more conodont specimens with muscle tissue are recovered so that destructive analysis can be undertaken. No evidence for a microspherical texture has been seen in eurypterid cuticle.

Although the initial clay mineral responsible for preserving the soft tissues may have been kaolinite, the composition is now illitic. Therefore, at some time between early diagenesis and discovery, the kaolinite must have gained K^+ and converted to illite. The K^+ may have come from the breakdown of any K-feldspars in the sediment at elevated temperatures and/or pressures. Illitization of kaolinite may take place at temperatures as low as 50 °C (Bjørkum and Gjelsvik 1988), but more usually occurs at intermediate burial depths (3–4 km) or elevated temperatures (130–150 °C) (Bjørkum and Gjelsvik 1988), both of which occurred in the Soom Shale. The reaction can be represented as:

$$\underset{\text{illite}}{KAl_3Si_3O_{10}(OH)_2} + 2SiO_{2(aq)} + H_2O \rightarrow \underset{\text{K-feldspar}}{KAlSi_3O_8} + \underset{\text{kaolinite}}{Al_2Si_2O_5(OH)_4} \tag{4}$$

where the direction of the reaction at low temperatures is determined by the degree of supersaturation of silica in the formation water with respect to quartz (Bjørkum and Gjelsvik 1988). However, for 100 °C and 300 bars, K-feldspar and kaolinite would have become unstable independent of silica activity, and K-feldspar and kaolinite would have reacted to form illite (muscovite) and quartz (Bjørkum and Gjelsvik 1988).

Organophosphatic fossils

The variable style in preservation of phosphatic fossils is problematical and at present only broad constraints can be placed upon the possible diagenetic pathways responsible. Lingulate brachiopods and conodont elements would have originally been composed of biomineralized calcium phosphate and organic components. Clays replaced at least some of the brachiopod shell but only the basal body of the conodont elements. How, then, are the different modes of preservation of these fossils with originally phosphatic-organic compositions accounted for?

The over-riding controls on the style of preservation in these fossils were the nature and configuration of the apatite crystallites and the abundance and position of the organics. Two diagenetic zones within the sediment may have existed: Zone 1, where the acidity was sufficient to begin to dissolve apatite, where clays existed as colloids and conditions may have been favourable for clay authigenesis, and below this, Zone 2, where the sediment began to lithify, colloidal clays were not present but pore waters were still corrosive to apatite. Note that these zones were transitional and occurred below the zone of calcium carbonate dissolution. In addition, colloidal clays would probably have been present in low abundances in the bottom waters and would have increased in abundance in the sediment pore waters.

Brachiopods. The shells are preserved in three dimensions, so replacement could not have taken place after complete dissolution of the calcium phosphate. The brachiopod apatite may have been partially dissolved in zone 1, allowing colloidal clays to coat and subsequently replace the organic portion within the shell. Williams and Cusack (1996) have shown that the living organophosphatic shells of Carboniferous lingulid contained an acidic, hydrophilic gel, glycosaminoglycan (GAG) as one of their organic components. These GAGs mediated clay mineral (kaolinite) formation in the shell as they were degrading (Williams and Cusack 1996). It is very likely that Ordovician discinoids would have had a lot of GAGs in their shells (Alwyn Williams, pers. comm. 1997) and this may have encouraged not only clay mineral formation but also replacement of the organic material by clays. In addition, the periostracum may have acted as an organic substrate on which clays nucleated. The clay replacements would have been unaffected by the more acidic conditions in the second zone, but any remaining apatite would have been dissolved, accounting for the mouldic clay mineral preservation seen in the majority of shells.

Conodont elements. The phosphate of the dentine in the basal body tissue was more susceptible to dissolution than the enamel, owing to its greater porosity, and so may have been largely dissolved early in zone 1. The organic portion of the dentine was then available to be replaced by clay minerals. However, the enamel only possesses a small proportion of organic material (1 wt %) and its crystalline nature protected this from colloidal clays. At greater burial depths (zone 2), the acidity increased to a level where the aprismatic enamel crown tissue could be dissolved to leave a mould. Finally, the prismatic enamel of the crown was replaced by silica; pseudomorphing of original prismatic crystallites (Text-fig. 3A, E) indicates that the silica is not a mould fill, but the result of a metasomatic replacement of apatite by quartz. The prismatic quartz crystallites do not show any signs of dissolution such as ragged or etched surfaces. This strongly suggests that the quartz did not originally replace the whole denticle, with subsequent dissolution leaving only the denticle base mineralized, but that quartz replaced the remaining apatite after and/or during its removal. The retention of void space in the elements indicates that the dissolution of apatite and replacement by quartz must have taken place not long before the sediment became lithified so that the void was not compacted. Alternatively, dissolution of apatite and replacement by quartz may have taken place relatively recently when the shale was exhumed. In any case, large scale dissolution of apatite from conodont elements has occurred. Very low pH conditions would have been necessary for this. A possible source of silica may come from the transformation of kaolinite to illite which yields silica into solution (Bjørkum and Gjelsvik 1988; see equation (4) above).

Alunite genesis

Alunite is one end member of this large group of isomorphous basic sulphates with the general formula $AB_3(SO_4)_2(OH)_6$ (Scott 1987). There is essentially complete solid solution between alunite ($KAl^{3+}{}_3$) and some other members of the group, the most common of which are jarosite (KFe^{3+}) and natroalunite ($NaAl^{3+}$). There is also a wide range of less common substitutions by other anions and cations in all available sites in the structure (Brophy *et al.* 1962; Dutrizac and Kaiman 1976; Scott 1987). End members are: alunite- $KAl_3(SO_4)_2(OH)_6$; jarosite- $KFe_3(SO_4)_2(OH)_6$; natroalunite- $NaAl_3(SO_4)_2(OH)_6$; natrojarosite- $NaFe_3(SO_4)_2(OH)_6$; gorceixite- $BaAl_3(PO_4)_2(OH)_5.H_2O$; crandallite- $CaAl_3(PO_4)_2(OH)_5.H_2O$; goyazite- $SrAl_3(PO_4)_2(OH)_5.H_2O$; and florencite- $CeAl_3(PO_4)_2(OH)_6.H_2O$.

Three hypotheses are available for the genesis of the alunite/crandallite associated with the fossils in the Soom Shale. It may have been derived from: (1) oxidation of pyrite during early diagenesis or weathering; (2) drying out of the regolith after intense weathering; or (3) intense weathering of apatite.

Although there is currently little evidence to determine the mechanisms for the genesis of the alunite/crandallite, the timing of the event may be constrained. If the alunite minerals were formed during a weathering process, they would be expected to be common throughout the sediment, but this is not the case. Four core samples and four fossil-bearing hand specimens from both Keurbos and Sandfontein were analysed using the electron microprobe and only three grains of alunite were found in a sample from Sandfontein. In addition, all core samples and hand specimens from both Keurbos and Sandfontein were analysed using XRD and only one sample showed alunite peaks (sample K1.2). Fossil material containing alunite comes from lingulate brachiopods, conodont elements, eurypterids and trilobites; compared with its occurrence in the sediment, it is relatively commonly associated with fossils. Indeed, the alunite in the sediment may also be associated with scattered fossil fragments. Evidence strongly suggests that the fossils have all been replaced by clay minerals at some time during early diagenesis. Therefore, if the fossil material and sediment were largely composed of clay minerals upon lithification, there would seem to be no reason for weathering to cause the alunite minerals to be preferentially associated with the fossils. It seems more likely that alunite minerals grew prior to or concurrently with the clay replacement of the fossils when the fossil composition was distinct from that of the matrix. One tentative suggestion for the genesis of the alunite may be through the oxidation of pyrite associated with the fossils at times of bottom water oxygenation. The DOP values indicate that at some periods the bottom waters of the basin were oxygenated. Fossils decaying on the sea floor or when shallowly buried may have been in close proximity to active pyrite formation, or may have acted as loci for pyrite genesis by producing an anoxic decay halo. An oxygenation event would have resulted in pyrite oxidation, with the sulphate necessary for alunite genesis becoming available. There is no evidence for this scenario and it is only introduced as one of several possibilities.

It remains possible that the crandallite may have been formed by the intense weathering of apatite (Flicoteaux and Lucas 1984). However, in the Soom Shale only the lingulate brachiopods and conodont elements, both of which have crandallite associated with them, were originally composed of apatite. In addition, the arthropods may have had concentrations of phosphate in their cuticle. Briggs and Kear (1993*b*, 1994) demonstrated that sufficient phosphate was concentrated in the cuticle of decapod shrimps for soft tissue phosphatization to occur, when the source of phosphorus was entirely from the shrimp itself. Crandallite is present in the eurypterid and trilobite exoskeletons although it is unlikely that they contained enough phosphate in their cuticles to produce the amount of crandallite present upon weathering. Therefore, the near ubiquity of crandallite in fossil material suggests that weathering of apatite is not responsible for crandallite genesis. Alternatively, the crandallite may have formed by the alteration during weathering of previously formed alunite by substitution of potassium by calcium and sulphate by phosphate; anion substitution is in evidence in Text-figure 5A where SO_3 against P_2O_5 has a high negative correlation coefficient ($R = 0{\cdot}88$). However, the genesis of alunite and crandallite (and related minerals) allied to some of the fossils in the Soom Shale remains enigmatic.

Is preservation in clay minerals unique to the Soom Shale?

Flocculation of clay minerals on to bacteria occurs naturally in lakes (Avnimelech *et al.* 1982; Ferris *et al.* 1987), and clay mineral-microbial interactions are well recorded in soil horizons (e.g. Burns 1979; Stotzky 1980). Clay minerals are ubiquitous in marine black shale deposits. So why should the known preservation of soft tissues by clay minerals be restricted to the Soom Shale?

It may well be that comparable preservation does occur, but has not been recognized. One of the problems with clay minerals is that they form an almost ubiquitous component of sediments, so clay analyses obtained on fossil material may have been discarded as being due to sediment contamination. They should now be treated more seriously. One other case in which clay minerals have been implicated in soft tissue preservation is the Burgess Shale.

The Burgess Shale. The mode of preservation of the often shiny fossils from the Burgess Shale has a history of debate. Whittington (1971) presented evidence that the fossils were at least partly carbonaceous; however, preservation was thought to involve clay minerals by Conway Morris (1986). Butterfield (1990) employed acid maceration techniques and obtained organic fossil films which are coated by aluminosilicate films, principally potassium and chlorite micas (Conway Morris 1990*a*). The term Burgess-Shale-type preservation was introduced by Butterfield (1990, 1994) to describe the taphonomic pathway responsible for exceptional organic preservation of non-mineralizing organisms in fully marine siliciclastic sediments. The preservation of organics without mineralization requires some process to act to terminate decay, in particular the autolytic degradation by the organism's own enzymes (Butterfield 1990, 1995). There is good evidence that adsorption of degradative enzymes on to and within clay minerals achieves this (Butterfield 1990, 1995; Keil *et al.* 1994). Although the principal taphonomic mode of the Burgess Shale biota is organic, there is some degree of early diagenetic mineralization (e.g. Bruton and Whittington 1983; Butterfield 1990, 1995; Budd 1993). The role of clay minerals in the preservation of Burgess Shale biota is still being debated (Butterfield 1996; Towe 1996).

A result of the determination of organic preservation may be that the rôle of the aluminosilicate films covering the organics has not been adequately researched. Clay minerals probably became aligned on the surface of the tissue before it decayed completely and, in this way, the outlines of organisms are preserved (Briggs *et al.* 1994). Other minerals, such as barium sulphate and cerium phosphate, have been reported in association with the aluminosilicate films (Conway Morris 1990*b*); analyses of these minerals have not been published but it is possible that they are alunite group minerals (gorceixite and florencite). In addition, the remains of some hard parts are unusual, being composed of clay minerals; the exoskeleton of *Olenoides* is preserved in chlorite, illite and mica, and other shelly remains which were also originally calcareous appear to have a broadly similar composition (Conway Morris 1986). This alteration is currently presumed to have taken place relatively late in the diagenetic history because cracking and fracturing of the fossils has occurred, probably due to overburden pressure (Conway Morris 1986).

It is possible that a similar adsorption and coating of clay minerals on to organics occurred in the Burgess Shale as has been described in this study for the Soom Shale. However, in the Soom Shale, adsorption and coating have, in most instances, progressed further so that the organic tissues are completely replaced by clay minerals. An exception is the sclerotized material of the conodont eye capsules which remains as organic films coated by clay minerals. This may suggest that scleratin is one of the most recalcitrant structural biopolymers and/or that it was not sufficiently reactive to encourage complete replacement. It is possible that the structural biopolymers constituting some of the Burgess Shale fossils were relatively inert and inhibited complete replacement. Nearly all of the Burgess Shale fossils preserve the outlines of the organisms and not their more labile and reactive organic biomolecules, such as the muscle tissue. Alternatively, the sediment, pore water, bottom water and Eh/pH conditions may have been different in the Burgess Shale and affected the degree of clay mineralization. The role of clay mineral-organic interactions in the preservation of the Burgess Shale fossils requires more study. Clay minerals may have performed more than one rôle, that of inhibiting degradative enzymes (Butterfield 1990, 1995), but may also have been involved in mineralizing and perhaps stabilizing the organic components.

CONCLUSIONS

Upon death, carcasses from the Soom Shale biota would have sunk at varying rates to the sea floor unless they were buoyed up either by air already within them (e.g. in the chambers of orthoconic nautiloids) or by decay gases. There is no evidence to suggest that any significant lateral transport of carcasses took place before they reached the sea floor. Sedimentological evidence for this comes from the fine-grained, millimetric laminations consisting of extremely distal turbidites and hemipelagites. Palaeontological evidence indicating an autochthonous biota that underwent negligible lateral transport includes (1) fully articulated fossils especially conodont bedding plane assemblages, although disarticulation does not always result from transport if the organism is freshly dead (see Allison 1986); (2) randomly oriented *Siphonacis*, which would have become aligned even in weak currents; (3) attachment to orthoconic nautiloids of brachiopods which might have become detached in a turbidity current; and (4) the preservation of soft tissues in the orthoconic nautiloids, which would have decayed during prolonged floating.

The substrate may have been soupy but this is unlikely because no fossils lie at an angle to bedding as, for example, in the Posidonia Shales (Martill 1993). However, it is possible that fossils were rotated to become bedding parallel upon compaction of the shale. At times when the bottom waters were oxygenated, carcasses lying on the sea floor would have been susceptible to scavenging as well as decay. However, bottom waters in the basin were probably anoxic for most of the time, when carcasses on the sediment surface would not have been scavenged and would have undergone decomposition mainly via sulphate reducing bacteria. The carcasses would therefore have had a greater preservation potential during times of anoxia. It should also be pointed out that the bottom-waters in the Soom Shale basin may have been quite cool given the reasonably high latitude (60° S), and this would have retarded the decay rate. It has been shown that a twofold increase in decay rate can be expected for a temperature rise of 10° C (Swift *et al.* 1979), and experiments (Briggs and Kear 1993*a*) have shown that decay decreases with lowered temperature.

Aragonite underwent very early dissolution, sometimes whilst still on the sea floor, and calcite probably dissolved at the same time or very soon after. Apatite dissolution occurred later, at approximately the same time as clay minerals were growing on to and replacing organic material. The labile soft tissues, such as muscle tissue, would have been mineralized rapidly post-mortem by clay minerals. More recalcitrant organics such as chitin, pseudochitin and scleratin were also mineralized to varying degrees; this possibly began at the same time as mineralization of muscle tissue or may have occurred later. The organic components of organophosphatic fossils such as conodont dentine and brachiopod shells, were replaced by clay minerals. After the process of clay mineral replacement had ceased, apatite dissolution continued and conodont crown tissue was removed. Finally, the most crystalline apatite with a low organic content from the denticle cores was replaced by silica, probably at the same time as illitization of kaolinite.

This unusual sequence of early diagenetic events was nearly entirely controlled by the composition of the organic and sediment matter supplied to the sea floor, which in turn controlled the Eh-pH conditions of the ambient waters. In addition, the basin did not have a strong circulation system, so mixing of the water was negligible. With a thickness of approximately 3500 m, 90 per cent. of the Table Mountain sediments are composed of supermature quartz (Visser 1974). The possible source-areas of the sands, deduced from compositional and textural analyses, is believed by Visser (1974) to have consisted largely (*c.* 60 per cent. of the area) of granite gneisses (Precambrian basement of the Namaqualand area), with subordinate input from sediments and lavas from the northern Cape Province. These gneisses and sediments would have undergone considerable mechanical and chemical erosion before deposition as the silts and muds of the Cedarberg Formation. The geochemistry of the sediment has been shown to have had an influence on the bottom and pore water Eh/pH conditions and hence on the mode of preservation of both hard and soft parts of the organisms. Perhaps one attribute, the very low pH, was of fundamental importance in producing the unusual taphonomy of much of the biota and, in particular, the preservation of soft tissues in clay minerals. A consequence of the source area consisting largely of granite gneisses, with subordinate sediment input, and in particular few carbonate rocks, may have been the low pH conditions attained in the Soom Shale sediment; there was insufficient carbonate to act as a pH buffer, and too few reactive iron oxides to fix the H_2S produced by the sulphate reduction of organic matter. The paucity of calcium carbonate may also reflect its increased solubility in colder waters. In addition, iron oxides may not have been extensively developed in the Ordovician due to the lack of terrestrial plants producing soil profiles. It is possible that other diagenetic minerals which may stabilize soft tissues, such as phosphate, pyrite and siderite, may have to be inhibited by low pH before clay minerals can mineralize the tissues. Whether the Soom Shale provided a unique environment in which fossilization occurred or represents an end member in a continuum of geochemical environments where soft tissues are preserved is still to be tested.

Acknowledgements. I am indebted to Prof. R. J. Aldridge and to Dr J. N. Theron for many helpful discussions, advice and reading manuscript proofs; RJA was particularly patient and helpful with the manuscript drafting. Professors J. D. Hudson and A. C. Dunham helped me enormously with the problems encountered with pyrite and clay minerals, respectively. Drs D. M. Martill, R. G. Clements, M. J. Norry, N. J. Butterfield and P. R. Wilby helped with reading sections of the manuscript and discussion of ideas. Professor D. E. G. Briggs is especially thanked for rigorously refereeing the manuscript and making it much more readable. R. Branson (SEM and photography), R. N. Wilson (electron microprobe), A. Smith (XRD), N. G. Marsh and R. Kelly (XRF) gave excellent technical support. Mr and Mrs J. N. Nieuwoudt, Keurbos Farm, and Mr and Mrs J. D. Kotze, Sandfontein, kindly allowed access to fossil localities. Financial support for this work was partly from NERC Research Grant GR9/957 to Professor Aldridge; SEG held a NERC research studentship (GT4/92/190/G), and is currently a PDRA on NERC Research grant GR3/10177 to Prof. Aldridge. I also acknowledge with thanks the facilities provided by the Geological Survey of South Africa, Cape Town.

REFERENCES

ALDRIDGE, R. J. and THERON, J. N. 1993. Conodonts with preserved soft tissue from a new Ordovician Konservat-Lagerstätte. *Journal of Micropalaeontology*, **12**, 113–117.

—— —— and GABBOTT, S. E. 1994. The Soom Shale: a unique Ordovician fossil horizon in South Africa. *Geology Today*, **10**, 218–221.

ALLISON, P. A. 1986. Soft-bodied animals in the fossil record; the role of decay in fragmentation during transport. *Geology*, **14**, 979–981.

—— 1988*a*. Konservat-Lagerstätten: cause and classification. *Paleobiology*, **14**, 331–344.

—— 1988*b*. Soft-bodied squids from the Jurassic Oxford Clay. *Lethaia*, **21**, 403–410.

—— 1988*c*. The role of anoxia in the decay and mineralization of proteinaceous macro-fossils. *Paleobiology*, **14**, 139–154.

AVNIMELECH, Y., TROEGER, B. W. and REED, L. W. 1982. Mutual flocculation of algae and clay. *Science*, **216**, 63–65.

BAAS, M., BRIGGS, D. E. G., VAN HEEMST, J. D. H., KEAR, A. J. and DE LEEUW, J. W. 1995. Selective preservation of chitin during the decay of shrimp. *Geochemica et Cosmochimica Acta*, **59**, 945–951.

BAILEY, S. W. 1988. Chlorites: structures and crystal chemistry. 347–404. *In* BAILEY, S. W. (ed.). *Reviews in mineralogy, hydrous phyllosilicates (exclusive of micas)*. Mineralogical Society of America, Washington, 725 pp.

BARKER, C. C and HURST, U. J. 1985. Authigenic kaolinite with fossil bacteria in Eocene kaolin. *Geological Society of America, Abstracts with Programme, Southeastern Section*, **17**, 79.

BAYLISS, P. 1975. Nomenclature of trioctahedral chlorites. *Canadian Mineralogist*, **13**, 178–180.

BERNER, R. A. 1970. Sedimentary pyrite formation. *American Journal of Science*, **268**, 19–42.

—— 1981. Authigenic mineral formation resulting from organic matter decomposition in modern sediments. *Fortschur Mineral*, **59**, 117–135.

—— 1984. Sedimentary pyrite formation: an update. *Geochimica et Cosmochimica Acta*, **48**, 605–615.

—— and RAISWELL, R. 1983. Burial of organic carbon and pyrite sulphur in sediments over Phanerozoic time: a new theory. *Geochemica et Cosmochimica Acta*, **47**, 855–862.

—— and RAO, J. L. 1994. Phosphorous in sediments of the Amazon River and estuary: implications for the global flux of phosphorous to the sea. *Geochemica et Cosmochimica Acta*, **58**, 2333–2339.

BJØRKUM, P. A. and GJELSVIK, N. 1988. An isochemical model for formation of authigenic kaolinite, k-feldspar and illite in sediments. *Journal of Sedimentary Petrology*, **58**, 506–511.

BRADDY, S. J., ALDRIDGE, R. J. and THERON, J. N. 1995. A new eurypterid from the late Ordovician Table Mountain Group, South Africa. *Palaeontology*, **38**, 563–581.

BRIGGS, D. E. G. and CLARKSON, E. N. K. 1989. Environmental controls on the taphonomy and distribution of Carboniferous malacostracan crustaceans. *Transactions of the Royal Society of Edinburgh: Earth Sciences*, **80**, 293–301.

—— and KEAR, A. J. 1993*a*. Decay and preservation of polychaetes: taphonomic thresholds in soft-bodied organisms. *Paleobiology*, **19**, 107–135.

—— —— 1993*b*. Fossilization of soft tissue in the laboratory. *Science*, **259**, 1439–1442.

—— —— 1994. Decay and mineralization of shrimps. *Palaios*, **9**, 431–456.

—— BOTTRELL, S. H. and RAISWELL, R. 1991*a*. Pyritization of soft-bodied fossils: Beecher's Trilobite Bed, Upper Ordovician, New York State. *Geology*, **19**, 1221–1224.

—— ERWIN, D. H. and COLLIER, F. J. 1994. *Fossils of the Burgess Shale*. Smithsonian Institution Press, Washington and London, 238 pp.

—— RAISWELL, R., BOTTRELL, S. H., HATFIELD, D. and BARTELS, C. 1996. Controls on the pyritization of exceptionally preserved fossils: an analysis of the Lower Devonian Hunsruck Slate of Germany. *American Journal of Science*, **296**, 633–663.

BROPHY, G. P., SCOTT, E. S. and SNELLGROVE, R. A. 1962. Sulphate studies 2: solid solution between alunite and jarosite. *American Mineralogist*, **47**, 112–136.

BRUMSACK, H. J. 1989. Geochemistry of recent TOC-rich sediments from the Gulf of California and the Black Sea. *Geologische Rundschau*, **78**, 851–882.

BRUTON, D. L. and WHITTINGTON, H. B. 1983. *Emeraldella* and *Leanchoilia*, two arthropods from the Burgess Shale, British Columbia. *Philosophical Transactions of the Royal Society of London, Series B*, **300**, 553–585.

BUDD, G. 1993. A Cambrian gilled lobopod from Greenland. *Nature*, **364**, 709–711.

BURMANN, G. 1969. Inkohlung und Mechanische Deformation. Abgehandelt am Erhaltungsz Organischer Mikrofossilien. *Zeitschrift fur Angewandte Geologie*, **15**, 355–364.

BURNS, R. G. 1979. Interactions of microorganisms, their substrates and their products with soil surfaces. 109–138. *In* ELLWOOD, D. C., MELLING, J. and RUTTER, P. (eds). *Adhesion of microorganisms to surfaces.* Academic Press, London, 216 pp.

BURNS, R. G. 1980. Microbial adhesion to soil surfaces: consequences for growth and enzyme activity. 249–262. *In* BERKELEY, R. C. W., LYNCH, J. M., MELLING, J., RUTTER, P. R. and VINCENT, B. (eds). *Microbial adhesion to surfaces.* Ellis Harwood Ltd, Chichester, 559 pp.

BUTTERFIELD, N. J. 1990. Organic preservation of non-mineralizing organisms and the taphonomy of the Burgess Shale. *Paleobiology*, **16**, 272–286.

—— 1994. Burgess Shale-type fossils from a Lower Cambrian shallow-shelf sequence in northwestern Canada. *Nature*, **369**, 477–479.

—— 1995. Secular distribution of Burgess-Shale-type preservation. *Lethaia*, **28**, 1–13.

—— 1996. Fossil preservation in the Burgess Shale – reply. *Lethaia*, **29**, 109–112.

CANFIELD, D. E. 1989. Reactive iron in marine sediments. *Geochemica et Cosmochimica Acta*, **53**, 619–632.

—— and RAISWELL, R. 1991. Pyrite formation and fossil preservation. 338–388. *In* ALLISON, P. A. and BRIGGS, D. E. G. (eds). *Topics in geobiology: taphonomy; releasing the data locked in the fossil record.* Plenum Press, New York and London, 560 pp.

—— RAISWELL, R., WESTRICH, J. T., REAVES, C. M. and BERNER, R. A. 1986. The use of chromium reduction in the analysis of reduced inorganic sulfur in sediments and shales. *Quarterly Journal of the Geological Society, London*, **124**, 149–155.

CARLSON, S. 1990. Vertebrate dental structures. 531–554. *In* CARTER, J. G. (ed.). *Skeletal biomineralization: patterns, processes and evolutionary trends.* Van Nostrand Reinhold, New York, 797 pp.

CHESSELET, P. 1992. Disarticulated remains of an Ordovician Metazoan from the Cedarberg Formation, South Africa: a re-interpretation of *Eohostimella parva* Kovács. *Palaeontology of South Africa*, **29**, 11–20.

CISNE, J. L. 1973. Anatomy of *Triarthrus* and the relationships of the Trilobita. *Fossils and Strata*, **4**, 45–64.

COCKS, L. R. M., BRUNTON, C. H. C., ROWELL, A. J. and RUST, I. C. 1970. The first Lower Palaeozoic fauna proved from South Africa. *Quarterly Journal of the Geological Society, London*, **125**, 583–603.

CONWAY-MORRIS, S. 1986. The community structure of the Middle Cambrian Phyllopod bed (Burgess Shale). *Palaeontology*, **29**, 423–467.

—— 1990*a*. Late Precambrian and Cambrian soft-bodied faunas. *Annual Review of Earth and Planetary Sciences*, **18**, 101–122.

—— 1990*b*. Burgess Shale. *In* BRIGGS, D. E. G. and CROWTHER, P. R. (eds). *Palaeobiology: a synthesis.* Blackwell Scientific Publications, Oxford, 583 pp.

CRAMER, F. H., RUST, I. C. and DIEZ DE CRAMER, M. D. C. R. 1974. Upper Ordovician chitinozoans from the Cedarberg Formation of South Africa. Preliminary note. *Geologische Rundschau*, **63**, 340–345.

DUTRIZAC, J. E. and KAIMAN, S. 1976. Synthesis and properties of jarosite-type compounds. *Canadian Mineralogist*, **14**, 151–158.

ELLIOT, T. 1991. Siliciclastic shorelines. 155–188. *In* READING, H. G. (ed.). *Sedimentary environments and facies.* Blackwell Scientific Publications, Oxford, 615 pp.

FERRIS, F. G., FYFE, W. S. and BEVERIDGE, T. J. 1987. Bacteria as nucleation sites for authigenic minerals in a metal-contaminated lake sediment. *Chemical Geology*, **63**, 225–232.

FISHER, I. S. J. and HUDSON, J. D. 1985. Pyrite geochemistry and fossil preservation in shales. *Philosophical Transactions of the Royal Society of London, Series B*, **311**, 167–169.

FLETCHER, M., LATHAM, M. J., LYNCH, J. M. and RUTTER, P. R. 1980. The characteristics of interfaces and their role in microbial attachment. 67–78. *In* BERKELEY, R. C. W., LYNCH, J. M., MELLING, J., RUTTER, P. R. and VINCENT, B. (eds). *Microbial adhesion to surfaces.* Ellis Harwood Ltd, Chichester, 559 pp.

FLICOTEAUX, R. and LUCAS, J. 1984. Weathering of phosphate minerals. 292–317. *In* NRIAGU, J. O. and MOORE, P. B. (eds). *Phosphate minerals.* Springer Verlag, Berlin, 442 pp.

FOLK, R. L. 1993. SEM imaging of bacteria and nannobacteria in carbonate sediments and rocks. *Journal of Sedimentary Petrology*, **63**, 990–999.

FORTEY, R. A. and THERON, J. N. 1995. A new Ordovician arthropod, *Soomaspis*, and the agnostid problem. *Palaeontology*, **37**, 841–861.

GABBOTT, S. E., ALDRIDGE, R. J. and THERON, J. N. 1995. A giant conodont with preserved muscle tissue from the Upper Ordovician of South Africa. *Nature*, **374**, 800–803.

GÄCHTER, R. and MEYER, J. S. 1993. The role of microorganisms in sediment phosphorous dynamics in relation to mobilization and fixation of phosphorus. *Hydrobiologia*, **53**, 112–131.

GRAY, J., THERON, J. N. and BOUCOT, A. J. 1986. Age of the Cedarberg Formation, South Africa and early plant evolution. *Geological Magazine*, **123**, 445–454.

HARRIS, R. H. and MITCHELL, R. 1973. The role of polymers in microbial aggregation. *Annual Review of Microbiology*, **27**, 27–50.

HELZ, G. R., MILLER, C. V., CHARNOCK, J. M., MOSSELMANS, J. F. W., PATTRICK, R. A. D., GARNER, C. D. and VAUGHAN, D. J. 1996. Mechanism of molybdenum removal from the sea and its concentration in black shales: EXAFS evidence. *Geochimica et Cosmochimica Acta*, **60**, 3631–3642.

HUNT, S. and NIXON, M. 1981. A comparative study of protein composition in the chitin-protein complexes of the beak, pen, sucker disc, radula and oesophageal cuticle of cephalopods. *Comparative Biochemistry and Physiology*, **68B**, 535–546.

INGALL, E. D., BUSTIN, R. M. and CAPPELLEN, P. V. 1993. Influence of water column anoxia on the burial and preservation of carbon and phosphorus in marine shales. *Geochimica et Comsochimica Acta*, **57**, 303–316.

JOPE, H. M. 1965. Composition of brachiopod shell. H156–H164. *In* MOORE, R. C. (ed.). *Treatise on invertebrate paleontology. Part H. Brachiopoda.* Geological Society of America and University of Kansas Press, Boulder, Colorado and Lawrence, Kansas, 521 pp.

KEIL, R. G., MONTLUCON, D. B., PRAHL, F. G. and HEDGES, J. I. 1994. Sorptive preservation of labile organic-matter in marine-sediments. *Nature*, **370**, 549–552.

KOVÁCS-ENDRÖDY, E. 1986. The earliest known vascular plant, or a possible ancestor of vascular plants in the flora of the Lower Silurian Cedarberg Formation, Table Mountain Group, South Africa. *Annals of the Geological Survey of South Africa*, **20**, 93–118.

KRAUSKOPF, K. B. 1982. *Introduction to geochemistry*. McGraw-Hill International Series in Earth and Planetary Sciences, Singapore, 617 pp.

LEVENTHAL, J. S. 1983. An interpretation of carbon and sulfur relationships in Black Sea sediments as indicators of environments of deposition. *Geochemica et Cosmochimica Acta*, **47**, 133–138.

LORD, C. J. 1982. A selective and precise method for pyrite determination in sedimentary materials. *Journal of Sedimentary Petrology*, **52**, 664–666.

LUCAS, J. and PRÉVÔT, L. 1981. Synthèse d'apatite á partir de matière organique phosphorée (ARN) et de calcite par voie bactérienne. *Compte Rendu Academie des Sciences de Paris, Série 2*, **292**, 1203–1208.

—— —— 1984. Apatite synthesis by bacterial activity from phosphatic organic matter and several calcium carbonates in natural freshwater and seawater. *Chemical Geology*, **42**, 101–118.

MACKENZIE, F. T. and GARRELS, R. M. 1966. Chemical mass balance between rivers and oceans. *American Journal of Science*, **264**, 507–525.

MACKIN, J. E. and ALLER, R. C. 1984. Dissolved aluminium in sediments and water of the East China Sea: implications for authigenic mineral formation. *Geochemica et Cosmochimica Acta*, **48**, 281–297.

MACQUAKER, J. H. S. 1994. A lithofacies study of the Peterborough Member, Oxford Clay Formation (Jurassic), UK: an example of sediment bypass in a mudstone succession. *Journal of the Geological Society, London*, **151**, 161–172.

MARTILL, D. M. 1988. Preservation of fish in the Cretaceous Santana Formation of Brazil. *Palaeontology*, **31**, 1–18.

—— 1990. Macromolecular resolution of fossilized muscle tissue from an elopomorph fish. *Nature*, **346**, 171–172.

—— 1993. Soupy substrates: a medium for the exceptional preservation of ichthyosaurs of the Posidonia Shale (Lower Jurassic) of Germany. *Kaupia: Darmstäder Beiträge zur Naturgeschichte*, **2**, 77–97.

—— and HARPER, L. 1990. An application of critical point drying to the comparison of modern and fossilized soft tissue of fishes. *Palaeontology*, **33**, 423–428.

MAYER, I. M. 1993. Surface-area control of organic-carbon accumulation in continental-shelf sediments. *Geochemica et Cosmochimica Acta*, **58**, 1271–1284.

McLAREN, A. D. and SKUJINS, J. 1968. The physical environment of microorganisms in soil. 3–25. *In* GRAY, T. R. G. and PARKINSON, D. (eds). *The ecology of soil bacteria.* Liverpool University Press, Liverpool, 681 pp.

MOORE, A. E. and MARCHANT, J. W. 1981. A preliminary note on two trilobites from the Soom Member, Table Mountain Group. *Transactions of the Geological Society of South Africa*, **86**, 51–54.

MÜLLER, K. J. 1985. Exceptional preservation in calcareous nodules. *Philosophical Transactions of the Royal Society of London, Series B*, **311**, 67–73.

—— and WALOSSEK, D. 1985. A remarkable arthropod fauna from the Upper Cambrian 'Orsten' of Sweden. *Transactions of the Royal Society of Edinburgh: Earth Sciences*, **76**, 161–172.

NORRY, M. J., DUNHAM, A. C. and HUDSON, J. D. 1994. Mineralogy and element fractionation during mudrock sedimentation. *Journal of the Geological Society, London*, **151**, 195–207.

PICKERING, K. T., MARSH, N. G. and DICKIE, B. 1993. Data report: inorganic major, trace and rare earth element analyses of the muds and mudstones from Site 808. 427–451. *In* HILL, I. *et al. Proceedings of the Ocean drilling Program, Scientific Results*, **131.**

PIETZNER, H., VAHL, J., WERNER, H. and ZIEGLER, W. 1968. Zur chemischen Zusammensetzung und Mikromorphologie der Conodonten. *Paläeontographica, Abteilung A*, **128**, 115–152.

RAISWELL, R. 1982. Pyrite texture, isotopic composition and the availability of iron. *American Journal of Science*, **282**, 1244–1263.

—— and BERNER, R. A. 1985. Pyrite formation in euxinic and semi-euxinic sediments. *American Journal of Science*, **285**, 710–724.

—— —— 1986. Pyrite and organic matter in Phanerozoic normal marine shales. *Geochemica et Cosmochimica Acta*, **50**, 1967–1976.

—— BUCKLEY, F., BERNER, R. A. and ANDERSON, T. F. 1987. Degree of pyritization of iron as a palaeoenvironmental indicator of bottom-water oxygenation. *Journal of Sedimentary Petrology*, **58**, 812–819.

—— CANFIELD, D. E. and BERNER, R. A. 1994. A comparison of iron extraction methods for the determination of degree of pyritization and the recognition of iron-limited pyrite formation. *Chemical Geology*, **111**, 101–110.

RUST, I. C. 1967. On the sedimentation of the Table Mountain Group in the Western Cape Province. Unpublished D.Sc. thesis, University of Stellenbosch.

—— 1981. Lower Palaeozoic rocks of southern Africa. 165–187. *In* HOLLAND, C. H. (ed.). *Lower Palaeozoic of the Middle East, eastern and southern Africa, and Antarctica.* John Wiley & Sons Ltd, Chichester, 331 pp.

SANTORO, T. and STOTZKY, G. 1967. Influence of cations on the flocculation of clay minerals as determined by the electrical sensitizing zone particle analyser. *Proceedings of the Soil Science Society of America*, **31**, 761–765.

SCOTT, J. H. and SYMONS, N. B. B. 1977. Dental mineralization mechanisms, enamel, dentine, cementum. *In Introduction to dental anatomy.* Churchill Livingstone, Edinburgh, 464 pp.

SCOTT, K. M. 1987. Solid solution in, and classification of, gossan derived members of the alunite-jarosite family, northwest Queensland, Australia. *American Mineralogist*, **72**, 178–187.

SKUJINS, J., PUKITE, A. and McLAREN, A. D. 1974. Adsorption and activity of chitinase on kaolinite. *Soil Biology and Biochemistry*, **6**, 179–182.

STOTZKY, G. 1980. Surface interactions between clay minerals and microbes, viruses and soluble organics, and the probable importance of these interactions to the ecology of microbes in soil. 231–248. *In* BERKELEY, R. C. W., LYNCH, J. M., MELLING, J., RUTTER, P. R. and VINCENT, B. (eds). *Microbial adhesion to surfaces.* Ellis Horwood Ltd, Chichester, 559 pp.

STÜRMER, W. 1970. Soft parts of cephalopods and trilobites: some surprising results of X-ray examination of Devonian Slates. *Science*, **170**, 1300–1302.

SWIFT, M. J., HEAL, O. W. and ANDERSON, J. M. 1979. *Decomposition in terrestrial ecosystems.* Blackwell, Oxford, 372 pp.

TARNEY, J. T. and MARSH, N. G. 1991. Major and trace element geochemistry of holes CY-1 and CY-4: implications for petrogenetic models. *In* GIBSON, I. J., MALPAS, J., ROBINSON, P. T. and XENOPHONTOS, C. (eds). Cyprus crustal study project: initial Report, Holes CY-1 and 1a. *Paper of the Geological Survey of Canada*, **90–20**, 133–176.

TAYLOR, S. R. and McLENNAN, S. M. 1985. *The continental crust: its composition and evolution. An examination of the geochemical record preserved in sedimentary rocks.* Geoscience texts. Blackwell Scientific Publications, Oxford, 312 pp.

TEIGLER, D. J. and TOWE, K. M. 1975. Microstructure and composition of the trilobite exoskeleton. *Fossils and Strata*, **4**, 137–149.

THENG, B. K. G. 1979. Developments in soil science. *Formation and properties of clay-polymer complexes.* Elsevier, Amsterdam and New York, 362 pp.

THERON, J. N., RICKARDS, R. B. and ALDRIDGE, R. J. 1990. Bedding plane assemblages of *Promissum pulchrum*, a new giant Ashgill conodont from the Table Mountain Group, South Africa. *Palaeontology*, **33**, 577–594.

—— and THAMM, A. G. 1990. *Stratigraphy and sedimentology of the Cape Supergroup in the Western Cape. Guidebook Geocongress 1990.* Geological Society of South Africa, 64 pp.

TOWE, K. M., 1996. Fossil preservation in the Burgess Shale. *Lethaia*, **29**, 107–108.

TRAVERSE, A. 1988. *Paleopalynology.* Unwin Hyman, Boston, 600 pp.

VELDE, B. and MEUNIER, A. 1987. Petrologic phase equilibria in natural clay systems. 423–458. *In* NEWMAN, A. C. D. (ed.). *Chemistry of clays and clay minerals.* Mineralogical Society Monograph, Longman Scientific and Technical and the Mineralogical Society, Harlow, 480 pp.

VISSER, J. N. J. 1974. The Table Mountain Group: a study in the deposition of quartz arenites on a stable shelf. *Transactions of the Geological Society of South Africa*, **77**, 229–237.

VOIGT, E. 1988. Preservation of soft tissues in the Eocene lignite of the Geiseltal near Halle/S. *Courier Forschungsinstitut Senckenberg*, **107**, 325–343.

WESTGATE, L. M. and ANDERSON, T. F. 1982. Extraction of various forms of sulphur from coal and shale for stable isotope analysis. *Analytical Chemistry*, **54**, 2136–2139.

WHITTINGTON, H. B. 1971. Redescription of *Marella splendens* (Trilobitoidea) from the Burgess Shale, Middle Cambrian, British Columbia. *Bulletin of the Geological Survey of Canada*, **231**, 1–21.

WILBY, P. R. 1993*a*. The mechanisms and timing of mineralization of fossil phosphatized soft tissues. Unpublished Ph.D. thesis, Open University.

—— 1993*b*. The role of organic matrices in post-mortem phosphatization of soft-tissue. *Kaupia: Darmstädter Beiträge zur Naturgeschichte*, **2**, 99–113.

—— BRIGGS, D. E. G. and RIOU, B. 1996. Mineralization of soft-bodied invertebrates in a Jurassic metalliferous deposit. *Geology*, **24**, 847–850.

WILLEMS, H. and WUTTKE, M. 1987. Lithogenese lakustriner Dolomite und mikrobiell induzierte Weichyeil-Erhartung bei Tetrapoden des Unter-Rotliegenden (Perm, Saar-Nahe-Becken, SW-Deutschlund). *Neues Jahrbuch für Geologie und Paläontologie, Abhandlungen*, **174**, 213–238.

WILLIAMS, A. and CUSACK, M. 1996. Lingulid shell mediation in clay formation. *Lethaia*, **29**, 349–360.

MACKAY, S. and CUSACK, M. 1992. Structure of the organo-phosphatic shell of the brachiopod *Discina*. *Philosophical Transactions of the Royal Society of London, Series B*, **337**, 83–104.

WUTTKE, M. 1983. Weichteil-Erhaltung durch lithifizierte Microorganismen bei mittelozänen Vertebraten aus den Ölschiefern der Grube Messel bei Darmstadt. *Senckenberg Lethaea*, **64**, 509–527.

SARAH E. GABBOTT

Department of Geology
University of Leicester
University Road
Leicester LE1 7RH, UK
e-mail SG21@le.ac.uk

Typescript received 4 February 1997
Revised typescript received 11 August 1997